

**Dynamics of Piezoelectric Cantilevered Beam at Higher Bending  
Mode for Wind Energy Harvesting**

*A Dissertation Submitted  
in partial Fulfillment of the Requirements  
for the Award of the Degree of*

**MASTER OF ENGINEERING**

**in**

**CAD/CAM Engineering**

by

**Ravneet Singh**

**801684010**

**Under Supervision of:**

**Dr. Ashish Purohit**

Assistant professor

Mechanical Engineering Department

**Dr. Rajendra Kumar**

Assistant professor

Mechanical Engineering Department



**THAPAR INSTITUTE**  
OF ENGINEERING & TECHNOLOGY  
(Deemed to be University)

**MECHANICAL ENGINEERING DEPARTMENT  
THAPAR INSTITUTE OF ENGINEERING & TECHNOLOGY  
(A DEEMED TO BE UNIVERSITY), PATIALA, PUNJAB  
July, 2018**

## CERTIFICATE

This is to certify that the work done in this thesis report title “**Dynamics of Piezoelectric Cantilevered Beam at Higher Bending Mode for Wind Energy Harvesting**” submitted in partial fulfilment of requirement for the award of master of engineering degree in CAD/CAM in the mechanical engineering department of Thapar Institute of Engineering and Technology, Patiala, is an authentic record of work carried out by me under the guidance of **Dr. Ashish Purohit** and **Dr. Rajendra Kumar**, Mechanical Engineering Department, Thapar Institute of Engineering and Technology, Patiala. The matter embodied in this report has not been submitted in any part or full to any other university or institute for the award of any degree.



**Ravneet Singh**

**Roll No. 801684010**

This is to certify that above declaration made by the student concerned is correct to the best of my knowledge and belief.



**Dr. Ashish Purohit**

**Assistant Professor,**

**MED**

**Dated: 16/08/2018**



**Dr. Rajendra Kumar**

**Assistant Professor,**

**MED**

**Dated: 16/08/2018**

*Dedicated to*  
*My Parents and My Sister (Avneet)*

## **Acknowledgement**

I would like to specially acknowledge and extend my heartfelt gratitude to all those who have helped me in completion of this seminar thesis report. With the biggest contribution, I would like to thank **Dr. Ashish Purohit** sir and **Dr. Rajendra Kumar** sir for their time, support and encouragement throughout course of this studies. I have learned so much from them and look forward to their continuous support future endeavours in life.

Lastly, I would also like to thank my parents for their years of unyielding love and encourage. They have always wanted the best for me and I admire their determination and sacrifice.



**Ravneet Singh**

## **Abstract**

In the present work, a numerical study of dynamics of a piezoelectric embedded cantilevered beam vibrating at higher bending mode is carried out. Electric power output from the vibrating structure is also investigated. The investigation is primarily focused for higher mode vibration response as during the natural wind/flow induced vibration (flutter instability), the structure vibrates in combination of higher bending modes. A mathematical model of a cantilever beam with single/multiple piezoelectric patches is developed and solved by modal super position approach. It is observed that during higher bending mode vibration, role of frequency of vibration has become more dominant than the amplitude of vibration.

**Keywords:** Cantilevered beam, piezoelectric material patch (PZT-patch), Higher bending modes, flow induced vibration, Euler-Bernoulli beam theory, modal super-position method, charge generation.

# Table of Contents

List of Figures.....	i
List of Tables .....	iii
Nomenclature.....	iv
CHAPTER1 INTRODUCTION.....	1
1.1 Flow Induced Vibration .....	1
1.2 Piezoelectric Material .....	2
Summary.....	4
Chapter 2 LITERATURE REVIEW.....	5
2.1 Introduction.....	5
2.2 Literature Review of Vibration .....	5
2.2 Literature Review of Energy Harvesting from The Vibrations.....	6
2.3 Literature Related to Mathematical Modelling (Stepped Beam). .....	10
2.4 Literature Review Related to Numerical Method .....	11
2.5 Summary .....	12
2.6 Observation from Literature Review .....	12
CHAPTER 3 OBJECTIVES AND METHODOLOGY .....	13
3.1 Introduction.....	13
3.2 Objectives.....	13
3.3 Methodology .....	13
3.3.1 Test Model and Properties of Test Model .....	15
3.3.2 Mathematical Modelling of Regular Beam .....	16
3.2.3 Dynamic Response of Cantilever Stepped Beam .....	18
3.2.4 Dynamic Response of Cantilevered Stepped Beam of Three Sections.....	20
3.2.5 Estimating The Charge Generation from Cantilevered Beam with Piezoelectric Material Patch.....	24
3.4 Validation of Methodology.....	25
Summary.....	27
CHAPTER 4 RESULTS AND DISCUSSION .....	28
4.1 Response of the Beam .....	30
4.1 Estimation of Charge Generation .....	40
4.2 Optimal Position of the Piezoelectric Patch Material Where Maximum Charge Generation Obtained.....	41
Summary.....	43
CHAPTER 5 CONCLUSION AND SCOPE FOR FUTURE WORK.....	44

5.1 Conclusions .....	44
5.2 Scope for The Future Work.....	45
References .....	46

## List of Figures

<b>Figure No.</b>	<b>Figure captions</b>
Figure 1.1	Flapping flag in air
Figure 1.2	Generation of voltage when piezo-structure is deformed
Figure 1.3	Configuration of PZT-layer
Figure 2.1	(a) Theoretical model (b) Human leg with test model
Figure 2.2	(a)linear PEH (b) nonlinear PEH (c) PEH with a magnetic oscillator
Figure 2.3	A prototype of the piezoelectric laminated generator
Figure 2.4	Stepped beam with varying cross- section
Figure 3.1	Flowchart representing the schematic of methodology
Figure 3.2	(a) cantilevered beam with piezoelectric material (b) cross-section of beam
Figure 3.3	Cantilevered beam
Figure 3.4	Sinusoidal force acting on cantilevered beam
Figure 3.5	Cantilevered beam with two sections
Figure 3.6	Cantilevered beam of three sections
Figure 3.7	Cantilevered beam with piezoelectric material patch
Figure 3.8	Response of simply supported beam with analytical solution. [Rao]
Figure 3.9	Response of beam with present methodology
Figure 4.1	Cantilevered beam with piezoelectric patch
Figure 4.2	Cantilevered stepped beam
Figure 4.3	(a)-(c) Natural modes of the beam
Figure 4.4	(a)Mode of vibration (b)Time response graph (c) frequency spectrum at 6 Hz
Figure 4.5	(a)Mode of vibration (b)Time response graph (c) frequency spectrum at 8 Hz
Figure 4.6	(a)Mode of vibration (b)Time response graph (c) frequency spectrum at 58 Hz

- Figure 4.7 (a)Mode of vibration (b)Time response graph (c) frequency spectrum at 62 Hz
- Figure 4.8 (a)Mode of vibration (b)Time response graph (c) frequency spectrum at 183 Hz
- Figure 4.9 (a)Mode of vibration (b)Time response graph (c) frequency spectrum at 186 Hz
- Figure 4.10 (a)Mode of vibration (b)Time response graph (c) frequency spectrum at 60 Hz and 186 Hz
- Figure 4.11 Actual dynamic response of the beam with 2 frequencies excitation
- Figure 4.12 (a)Mode of vibration (b)Time response graph (c) frequency spectrum at 7 Hz, 60 Hz and 186 Hz
- Figure 4.13 Actual dynamic response of the beam with 3 frequencies excitation
- Figure 4.14 Cantilevered stepped beam
- Figure 4.15 Strain produced along the beam during deflection
- Figure 4.16 Various location of PZT-patch
- Figure 4.17 Cantilevered beam with PZT-patch at distance  $x$
- Figure 4.18 Graph of charge against position of PZT-patch

## List of Tables

<b>Table No.</b>	<b>Table Captions</b>
Table 3.1	Properties of test models (Beam and PZT-patch)
Table 4.1	Shows the property of beam and PZT patch used for the analysis.
Table 4.2	Corresponding three natural frequencies of the equivalent beam
Table 4.3	Properties of different section in cantilevered beam
Table 4.4	Shows the amount of Charge generation

## Nomenclature

M	Mass matrix
K	Stiffness matrix
$f_1(t)$	Free excitation
$f_2(t)$	Forced excitation
$Q$	Charge
$D_z$	Displacement in $z$ -direction
$b$	Width of the beam
$e_{31}$	Piezoelectric constant
$E_z$	Electric field
E	Young's modulus
L	Length of beam
$T_b$	Thickness of beam
$T_p$	Thickness of PZT-patch
$I_b$	Moment of inertia of beam
$I_p$	Moment of inertia of PZT-patch
$A_b$	Cross-section area of beam
$A_p$	Cross-section area of PZT-patch
$B_b$	Width of the beam
$B_p$	Width of PZT-patch
$EI$	Flexural rigidity
$x$	Longitudinal coordinate
$w$	Deflection of beam
$f(t)$	External force vector
$t$	Time vector
N	Number of modes
F	Sinusoidal force
$\omega_n$	Natural frequency of beam
X	Distance of PZT-patch from fixed end

## Greek Symbols

$\epsilon_x$	Strain
$\epsilon_{33}$	Dielectric constant
$\rho$	Density of material
$\varphi_i(x)$	$i^{th}$ mode shape of the un deformed beam
$\eta_i(\tau)$	Modal coordinate

# CHAPTER 1

## INTRODUCTION

---

Present days belief holds the utilization of the term energy harvesting or energy scavenging to depict the phenomenon by which energy is harvested from surrounding assets such as wind, sun powered radiation, warm inclination and vibrations/movements to be either conserved or utilized straightforwardly to control low-vitality gadgets. This field has seen extensive concern in recent years due to development in wireless and micro electro-mechanical systems (MEMS) technology that has forced the interest for another period of portative hardware and remote sensors. So energy harvesting from vibrations is one of the most abundant source i.e. available from day to day life or any other mechanical operations.

Vibrations can be produced from many sources such as wind, is the one of the most sustainable and easily available ambient resource. When an elastic structure exhibits in a flow it loses its stableness hence starts vibrating. Phenomenon of vibration produced by flow is known as “Flow induced vibrations”. Combination of flow induced vibrations and piezoelectric material have a great boon for the field of energy harvesting. Researchers have found that the longer the flexible structure is, the larger the its deformation would be. At the same time, piezoelectric devices are being attached in order to harvest energy due to the ability to convert mechanical energy into electrical energy. When the mass and elastic properties of the structure are suitable, the vortex street built behind the body generates forcible oscillations in the structure that can be transformed into electricity. Different geometry is used by different authors however cantilever geometry is commonly used structure in the piezoelectric energy harvesters, specifically for the mechanical energy harvesting from vibrations. Moreover, mechanical strain can be created within the piezoelectric during the vibration and hence, electric charge is developed. In the present dynamic behaviour and subsequent charge generation from a cantilevered beam with piezoelectric material are studied.

### 1.1 Flow Induced Vibration

When the flowing fluid interacts with a flexible structure in its way, the unsteady fluid pressure excites the structure into dynamic motion. The flow-induced vibration primarily involves two types of excitation mechanisms, free excitation and forced excitation. Following

equation demonstrates the equation of motion of flow-induced vibration of a one degree of freedom system.

$$m\ddot{x} + kx = f_1(t) + f_2(t)$$

where,  $m$  is the mass of system,  $k$  is stiffness. The unsteady force from the flow is separated into two parts and represented by functions  $f_1(t)$  and  $f_2(t)$ , which are corresponding to the free and force excitation respectively. In the case of free vibration ( $f_1(t) \neq 0$ ,  $f_2(t) = 0$ ), there is no external excitation and the motion of the structure is purely due to the instability induced by the wake shed from the structure itself. Such problems are categorized as movement induced excitation (MIM) [leung et al.]. A typical example of free vibration is aero elastic flutter in the flags or plates, where the excitation is a function of structural motion itself [Paidoussis]. Conversely, the force excitation ( $f_1(t) = 0$ ,  $f_2(t) \neq 0$ ) belongs to a class of problems where the force is originated by the external turbulence and gust (extraneously induced excitation, EIE), or by the unsteady vortical field present in the flow stream (Vortex-induced vibration, VIV). A flexible plate with an upstream bluff body is a benchmark model to demonstrate vortex-induced vibration phenomenon. We observe a flag flapping in the air as shown in Figure 1.1 is the example, which demonstrate the phenomenon of flow induced vibrations.

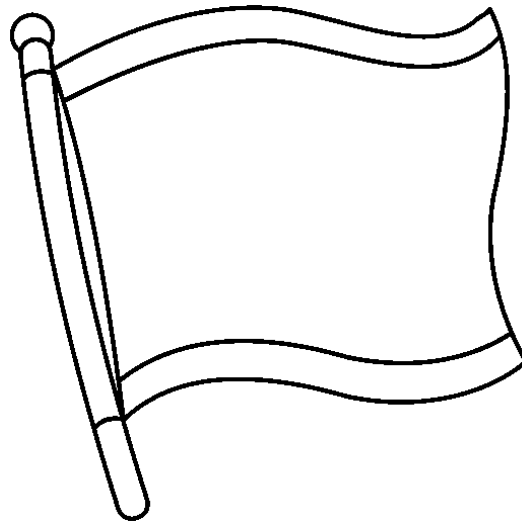


**Figure 1.1 Flapping flag in air**

## 1.2 Piezoelectric Material

The word emerges from the Greek word “piezein”, which signify “to press”. Discovered in 1880 by Pierre curie in quartz crystals. Piezoelectric are materials that can produce electricity when exposed to a mechanical stress. Piezoelectric material will also do operation in reverse,

inducing strain by the employment of electric field. Piezoelectric material generates voltage when piezo material structure is deformed as shown in Figure 1.2.

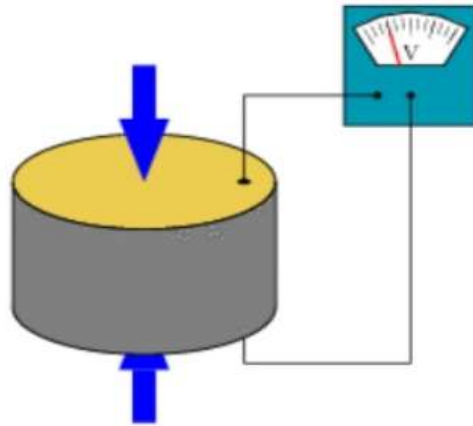


**Figure 1.2 Generation of voltage when piezo-structure is deformed**

According to previous research study a most of the piezoelectric energy harvesting devices implies two configurations i.e. first is unimorph configuration as shown in Figure 1.3(a) in which piezoelectric patch have been bonded to the one side of cantilever beam and other is bimorph configuration as shown in Figure 1.3(b) in which piezoelectric patch bonded to the both sides of cantilever beam. In the present study the cantilever beam with unimorph configuration has been investigated and all the results are properly analysed.

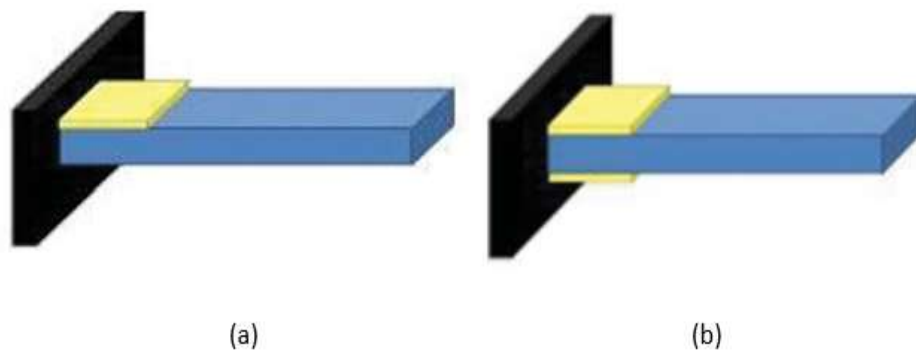


**Figure 1.3 Configuration of PZT-layer**

A thin layer of piezoelectric materials can be put into a cantilever and appended into it with a non-piezoelectric layer (normally metal or steel assumes a part as a conveyor of the produced charge), and having its one end fixed keeping in mind the end goal to actualize the bending mode of the structure. Researches are still going on how to enhance the performance of piezoelectric materials so they can generate more energy for the further use.

Piezoelectric materials can be regular or man-made. The regular PEM are gem materials like quartz ( $\text{SiO}_2$ ), Rochelle salt, Topaz, Tourmaline-gather minerals and some natural substances as silk, wood, polish, dentin, bone, hair, elastic. Man-made PEM are additionally called manufactured PEM and its composes are lead zirconate titanate(PZT), Zinc oxide( $\text{ZnO}$ ), Barium titanate ( $\text{BaTiO}_3$ ) and Lead titanate( $\text{PbTiO}_3$ ) etc. The various advantages or properties that enhance the use of piezoelectric material in vibrating structure for energy harvesting:

1. Unaffected by outside electromagnetic fields.
2. Pollution free.
3. Low maintenance.
4. Easy substitution of equipment.

**Application:**

1. Energy generation or energy harvesting.
2. Industrial Applications like Pressure Sensors, Sonar Equipment and Diesel Fuel Injectors etc.
3. Defence Applications like Micro Robotics and Course-changing Bullets.
4. Medical Applications like Ultrasound Imaging and Ultrasonic Procedures.

**Summary**

The increased use of piezoelectric material along with flexible structure have encouraged the researcher to predict the maximum deflection of the cantilever beam at various location which results maximum strain or generates maximum charge from the piezoelectric material patch. In the present work, the focus of the work is to understand the electro-mechanical effect of piezoelectric layer while vibrates under the mixed mode condition. However, to make process less complicated, instead of exciting the plate by the actual flow field, which required to solve complex governing equation of flow field, direct excitation to the plate is employed. It may be noted that the given excitation causes plate to vibrate in combination of multiple modes, which is observed during the case of flow induced vibration. In addition, a parametric study to obtained most effective location of the piezoelectric layer on the base cantilevered plate is also carried out.

## CHAPTER 2

### LITERATURE REVIEW

---

#### 2.1 Introduction

The energy harvesting with piezoelectric material have been investigated by many ways in the past. Various test models and methods have been used to harvest the energy with piezoelectric material during three last decades.

In the present research study, literature review is based upon three categories: -

- I. Vibration/flow induced vibration of plane structures.
- II. Energy harvesting from vibrations of structures.
- III. Analytical/numerical solution of beam.

Eloy *et al.* (2008) have been investigated on Aero elastic unsteadiness of cantilevered elastic plates in regular flow. Researchers have been stated that flutter unstableness of an elastic plate mainly depends upon the two things first one is pressure force and second one is bending stiffness and they concluded that two-dimensional limit cannot be accomplished by experimentation because hysterical manner and three-dimensional cause arise for plates of large aspect ratio.

Balint *et al.* (2005) have been studied the stableness of a cantilevered elastic plate in viscous channel flow. Investigation of an elastic cantilevered plate in viscous flow is examined as a description of the dynamics of the human upper airway. The aim is on the unstableness mechanisms of the soft plate (flexible plate) that results airway blockage while sleeping. They have been solved the Navier–Stokes equations for flow with Reynolds numbers up to 1500 fully linked with the deflection of the plate motion explained using finite-differences.

Allen *et al.* (2001) have been studied the probability of placing the piezoelectric or “eel” in the wake of an abrupt structure and by adopting the von Karman vortex street making behind the abrupt structure to generate oscillations in the structure. The oscillations which build up the capacitance in the membrane that generates a voltage source.

Tang *et al.* (2009) have been done and investigation that cantilevered elastic plate in axial flow usually lack of its steadiness by flutter. In the time-domain investigation accomplished to this end, the wake behind the oscillating cantilevered plate is presumed to affair tangentially from

the free trailing edge and enlarge downstream with a swinging form is shown that the wake has been less impact on system stability for long plates than it does for short ones.

Akaydin *et al.* (2010) have been identified some features of energy harvesting from irregular turbulent fluid flow using piezoelectric generators. Turbulent flows depict a huge degree of consistency in the spatial and temporal scales, which gives a best chance for energy harvesting. The voltage induced by short, elastic piezoelectric cantilevered beams bonded inside turbulent boundary layers and wakes of circular cylinders at high Reynolds numbers is studied. Their simulation results had a best agreement with the experiment data covering the way of using such a method to approximate the production of different energy gathering devices within unsteady flow fields.

Huang *et al.* (1995) have been explored the ripple of cantilevered plates in hub liquid stream. They researched the consistent quality of the plate through an underlying worth issue. Theodor Sen's traditional arrangement has been embraced for the liquid stacking however consistency has been unequivocally barred. Nonetheless, its impact has been implanted in the kutta-Zhukovskii condition. Direct examination has been picked in light of the fact that the primary intrigue lies in the underlying phase of instability. An indicator corrector numerical strategy has been created to re-enact the transient procedure which prompting the long haul occasional conduct. In the present investigation, they inferred that the limit dependability can be broadened significantly more by hardening the plate which has added to accomplish a superior come about for relieving snoring.

## 2.2 Literature Review of Energy Harvesting from The Vibrations

Izadgoshasba *et al.* (2018) have contemplated that a cantilevered pillar with a piezoelectric layer reinforced toward the finish of the shaft was assessed for potential to assemble vitality from human strolling. The impact of introduction of the cantilevered shaft with end tip mass on the adequacy of the power created has been tentatively examined. Two models appeared in Figure 2.1 were produced one was associated onto the leg of a human strolling on a treadmill at a uniform speed and another has been hypothetical lumped show utilized to appraise the voltage yield utilizing the explored estimated quickening. They presumed that outcomes portray great concurrence with the examination and the model. As in additionally considers scientists inferred that the most extreme power has been discovered when the PEH

(Piezoelectric vitality gatherer) has been balanced at  $70^\circ$  with reference to a facilitate framework associated with the leg when individual strolling done on a treadmill.

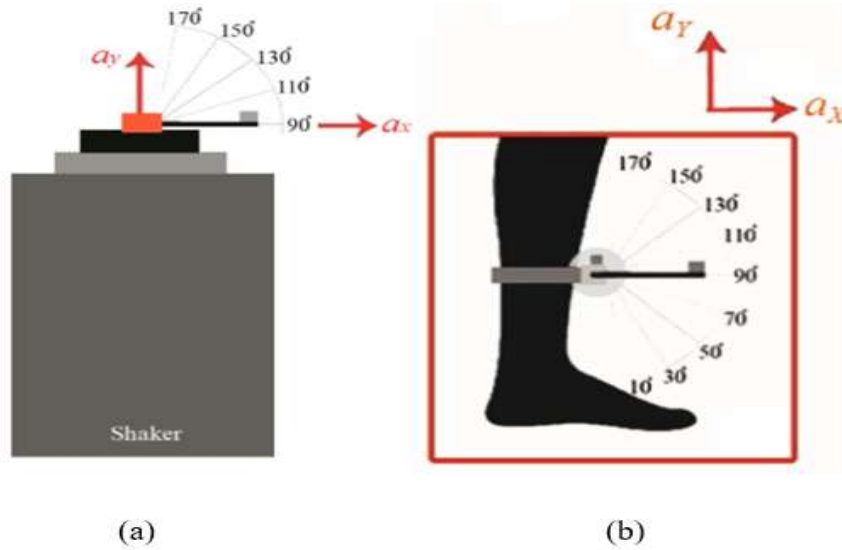


Figure 2.1 (a) Theoretical model (b) Human leg with test model

Tang *et al.* (2012) has been introduced a new method i.e. magnetic linked piezoelectric energy harvester (PEH) as shown in Figure 2.2, in which the magnetic interaction has been introduced by a magnetic oscillator. Three models have been studied which are conventional linear PEH, the nonlinear PEH with an engaged magnet, and the developed PEH with a magnetic oscillator. In the further investigation they concluded that by using magnetic oscillator, 41% of increment in the magnitude of the power generating output has been obtained at an excitation level of 2 m/s.

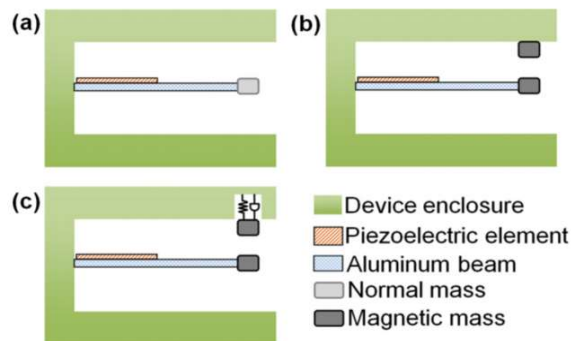
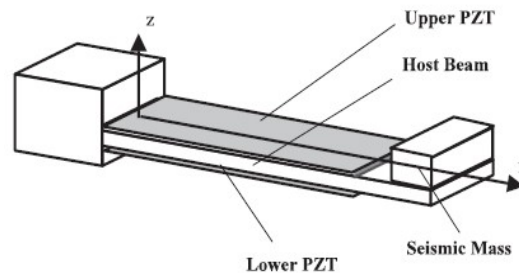


Figure 2.2 (a)linear PEH (b) nonlinear PEH (c) PEH with a magnetic oscillator

Akaydin *et al.* (2010) have been identified some features of energy harvesting from irregular turbulent fluid flow using piezoelectric generators. Turbulent flows depict a huge degree of consistency in the spatial and temporal scales, which gives a best chance for energy harvesting. The voltage induced by short, elastic piezoelectric cantilevered beams bonded inside turbulent boundary layers and wakes of circular cylinders at high Reynolds numbers is studied. Their simulation results had a best agreement with the experiment data covering the way of using such a method to approximate the production of different energy gathering devices within unsteady flow fields.

Kumar *et al.* (2016) have been contemplated the demonstrating and outline of a Cantilever Beam for Piezoelectric Energy Harvesting on which Piezoelectric layer of Lead Zirconate Titanate(PZT) patches are joined. Two setups have been utilized one is "Unimorph" in which just a single PZT fix and the other is "Bimorph" in which two PZT fix are connected to the pillar. Euler Bernoulli shaft hypothesis have been utilized for contemplated the dynamic reaction of pillar. Demonstrating of the bar is finished by limited component strategy. Three area of PZT patch(s) have been considered i.e. close to the settled end of the bar, close to the free end and amidst the shaft. Excitation have been given by as consonant sinusoidal power and every one of the activities have been done in the main method of vibration. In the further examination they presumed that best outcome has been gotten when the piezoelectric layer is attached close to the fixed end.

Lu *et al.* (2003) have studied the very small size of the remorable such as (MEMS) and compose them broadly eligible for some special cases. In this investigation, a common impression of the piezoelectric energy conversion has been studied. A simple design modelling and analysis of the '31' transverse mode type piezoelectric micro-generator is introduced as shown in Figure 2.3.



**Figure 2.3 A prototype of the piezoelectric laminated generator**

Two case studies of laminated type micro-generators which are PZT-PIC 255 and PZN-8% PT have been studied and results are compared. The output power generated by two case studies

has been studied in the form of charge. The output power (charge) have been calculated by following formula.

$$Q = \int_A D_z dA = b \int_{L_0}^{L_1} (e_{31} \varepsilon_x + \epsilon_{33} E_z) dx$$

Where  $Q$  is charge,  $D_z$  is displacement in  $z$ -direction,  $b$  is the width of the beam,  $e_{31}$  is the piezoelectric constant,  $\varepsilon_x$  is strain generated along beam,  $\epsilon_{33}$  is the dielectric constant  $E_z$  is the electric field.

Erturk *et al.* (2009) examined displaying of cantilevered piezoelectric vitality collectors under base excitation. The bimorph cantilever setups with arrangement and parallel associations of piezo earthenware layers was explored by applying the logical arrangement. The suspicion for base excitation was taken as the interpretation the transverse way with a superimposed little pivot. The voltage yield and vibration reaction to translational and rotational base increasing velocities was relate utilizing electromechanical recurrence reaction capacities (FRFs) and distinguished from the multi-mode and single-mode arrangements. In the further examination creators approve the exploratory model of the single-mode coupled voltage yield and vibration reaction articulations for a bimorph cantilever with a tip mass and they presumed that the forecast for the coupled framework progression for an extensive variety of electrical load obstruction should effectively be possible by shut shape single-mode FRFs gained from the systematic arrangement and execution for the short out and open circuit reverberation recurrence excitations of the bimorph gadget was dissected broadly and in addition for show precision.

Wang *et al.* (2000) had been showed their concern with the optimal design of a collocated pair of piezoelectric patch actuators that are surface bonded onto beams. The study was based upon selecting the optimal locations and sizes (or lengths) of the piezoelectric actuators by the selecting criteria of a controllability perspective. The obtained controllability index depends on the placement and size of the piezoelectric patches, and thus maximizing the value of index the designer can obtained the optimal design of the piezoelectric actuator.

Friswell *et al.* (2012) purposed another arrangement for a cantilevered beam comprising a tip mass settled vertically and energized the transverse direction at its base. The electromechanical conditions of movement for the specified framework were created, and its reaction was watched for a scope of parameters utilizing stage pictures and bifurcation outlines. At that point

they built up a test demonstrate and contrasted their outcomes and reproducing information and they reasoned that it demonstrated a good agreement.

Bailey *et al.* (1985) outlined a functioning vibration damper for a cantilever pillar utilizing a dispersed parameter actuator and appropriated parameter control hypothesis. The appropriated parameter actuator was a piezoelectric polymer, poly (vinylidene fluoride). Lyapunov's second technique for circulated parameter frameworks was executed to plan a control calculation for the damper and they inferred that all methods of a shaft can be at the same time control if the precise speed of the tip of the bar is known. Primer testing of the damper was performed on the principal method of the cantilever bar demonstrates an extraordinary effect control on the vibration of the cantilevered beam.

Bilgen *et al.* (2013) talked about the electromechanical effectiveness and power yield limit of a rearranged cantilevered bar vibration vitality collector with a tip mass within the presence of unadulterated harmonic, pure random and different mixes of harmonic and irregular base excitation cases. The composite piezoelectric material gadget was associated close to the foundation of the bar. The tip mass was utilized to start the non-linearity of the framework by prompting locking in a few arrangements and maintaining a strategic distance from it in others. The test investigation and results demonstrates the great concurrence with the numerical simulations.

### 2.3 Literature Related to Mathematical Modelling (Stepped Beam)

Kisa *et al.* (2007) presented another numerical procedure connected to the uniform and ventured broke shafts with roundabout cross segment for examining the free vibration. The Finite Element and Component Mode Synthesis strategies was connected together and the shaft was isolated into parts from the break segment. The different numerical cases were inspected with the expectation of complimentary vibration examination of bars with transverse non-engendering open breaks to confirmed the presented strategy. In the further examination, creators have been confirmed the technique which was suitable for the vibration investigation of uniform and ventured split bars with roundabout cross section.

Junior *et al.* (2016) proposed a scientific displaying which depended on Euler-Bernoulli shaft hypothesis for a ventured pillar on flexible end underpins. The characteristic frequencies and mode states of a ventured bar were considered and contrasted and each other. Different Combinations of the ventured bar i.e. established clasped, stuck, sliding, and free kinds of versatile end bolsters are considered. In the further examination, initial three recurrence

parameters of shafts with two stage changes in cross-segment are classified. In additionally examine consider, analysts proposed a technique to decide the initial three characteristic recurrence of the ventured bar with differing cross-area as appeared in Figure 2.4.

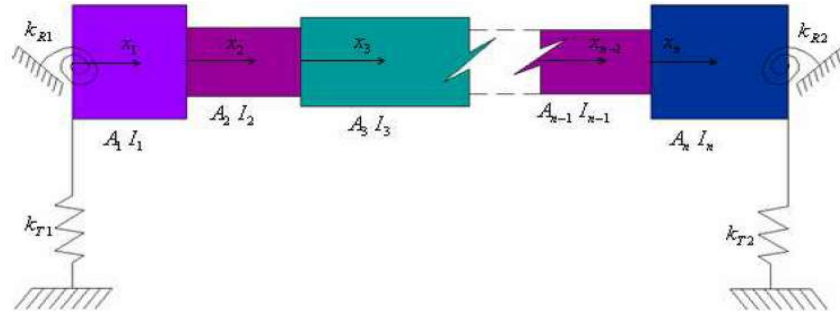


**Figure 2.4 Stepped beam with varying cross- section**

Jang *et al.* (1989) have been resolved the most minimal regular recurrence of a ventured bar with two distinctive cross-segments is looked for different limit conditions. In the further examination correct arrangements have been computed and are contrasted. The outcomes acquired by the utilization of the limited component technique such as finite element method with non-number polynomial shape capacities and with a code, MSC/PAL.

## 2.4 Literature Review Related to Numerical Method

Godara *et al.* (2018) considered a feedforward control technique for smothering the contact bobs in electrostatically determined small scale switches. Built up a scientific model which incorporates the impacts of mid-plane extending, bordering field capacitance, crush film damping and furthermore the impact of flexible contact with the stationary dielectric substrate. Incomplete differential conditions of electrostatic switch were discretized into customary differential conditions utilizing Galerkin's technique. Both arrangement i.e. fixed– settled and fixed– free of the switch, strength and adequacy of the strategy have been researched.

Godara *et al.* (2016) examined a feedforward control procedure for lightening the lingering motions in electrostatically determined no prismatic microbeams. The overseeing differential condition has been created. Modular superposition strategy with full-arrange electrostatic nonlinearity have been utilized to fathom the condition of movement numerically. A feed-forward control procedure was proposed to diminish the impact of lingering motions; in this manner accomplishing quick exchanging between the progressive harmony designs. The impact on the execution of the proposed control methodology because of the high vibration modes was additionally contemplated.

Godara *et al.* (2015) examined the advancement of a charge forming strategy for alleviating such leftover motions in electrostatically incited miniaturized scale pillars and accomplishing quick exchanging between the progressive balance states. The strategy for modular superposition was utilized to get the dynamic reaction of small scale bars. The significance of the proposed method was exhibited by thinking about an extensive variety of differing parameters in the groupings of geometric nonlinearity, damping, and equilibrium.

## 2.5 Summary

In the context of energy harvesting from the vibrations researchers have been worked in many ways like flow induced vibration, shaker operations etc. Different methods have been used for the energy scavenging like test model of beam attached to the human leg during the walking motion on treadmill, magnetic exciter attached to the casing for increment in amplitude of vibration for maximum energy generation, introducing the tip mass to the end of beam. For energy extraction from vibration various numerical have been explored by many researchers like finite element method, finite difference method and some analytical solutions have been also adopted like modal super-position method etc.

## 2.6 Observation from Literature Review

The literature available in the context of energy harvesting from vibration and following observations are made:

1. It has been noted that in most of the previous work related to energy harvesting from vibration of a cantilevered beam using piezoelectric material focused for first bending mode of the beam. However, study of such energy generation for higher bending mode is limited.
2. Role of both amplitudes of vibration and frequency of vibration on the generation of electric charge were investigated, however, influence of higher modal frequency of the structure has not been explored in detail.
3. Extraction of energy using piezoelectric material from the flow induced vibration is while the structure vibrates under mixed mode is limited.

# CHAPTER 3

## OBJECTIVES AND METHODOLOGY

---

### 3.1 Introduction

From the review of literature, it has been observed that during the instable flow induced, vibration structure undergoes/exhibits vibration in mixed mode, generally first few modes appears simultaneously [Tang *et al.*] and significant research carried out in past to understand complex phenomenon. However, it is noted that in the research of energy generation from this vibration of plane structure, mainly first bending mode is considered and energy generation while the structure vibrating in the higher bending mode is not explored. Thus, the primary intension of the present study is to investigate the energy generation from a plane structure (charge generation) while it is vibrating in the higher bending modes. It may be noted that in actual phenomenon of FIV, excitation is originated by the unsteady fluid forces, however, in the present study, the structure is excited virtually by combination of higher frequencies and following charge generation is calculated

### 3.2 Objectives

Following objectives have been coined based on the observation noted in the literature review.

- I. Study of dynamic response of cantilevered beam with excitation of higher modal frequency.
  - a. Euler-Bernoulli beam theory is employed as governing equation.
  - b. Numerical/ analytical solution of governing equations.
- II. Investigation of cantilevered beam of uniform thickness and non-uniform thickness with piezo-electric patch along the length of the beam.
  - a. A mathematical modelling of a cantilever beam with uniform thickness and non-uniform thickness is done by using modal-superposition approach.
- III. Electric power output from the vibrating structure and Optimal placement for higher charge generation along with piezo-patch is also studied along the length of beam.

### 3.3 Methodology

In this section, methodology of the present study is discussed. For the energy generation from smart material, as a base structural a cantilevered beam with a piezoelectric patch is considered.

For the investigation of dynamic response of the beam, Euler- Bernoulli beam for a variable shape beam is employed. The governing equation is solved by modal super position approach. Flowchart as shown in the Figure 3.1 represents the schematics of the methodology.

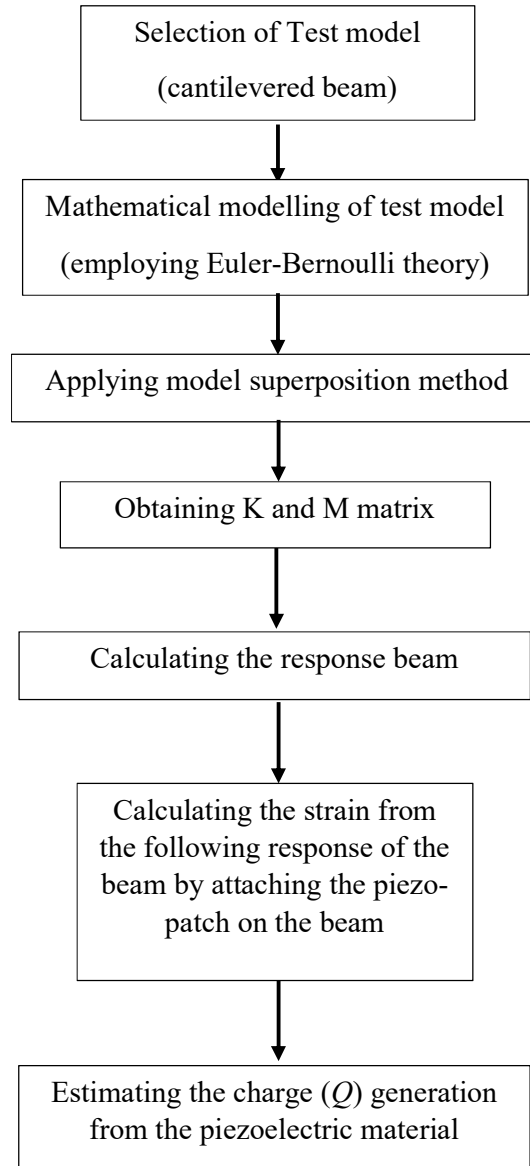


**Figure 3.1** Flowchart representing the schematic of methodology

### 3.3.1 Test Model and Properties of Test Model

A Cantilever beam bonded with PZT patch(s) also known as smart beam, is used as test model as shown in Figure 3.2. Table 3.1 shows the test model property of beam and PZT patch [Lu *et al*] which is used in present study as test model.

**Table 3.1 Properties of test models (Beam and PZT-patch)**

<b>Property</b>	<b>Test models</b>	
	<b>Beam</b>	<b>PZT-Patch</b>
<b>Young's modulus</b>	210GPa	63GPa
<b>Density</b>	7800 Kg/m <sup>3</sup>	7500 Kg/m <sup>3</sup>
<b>Length</b>	0.3m	0.1m
<b>Width</b>	0.03m	0.03m
<b>Thickness</b>	0.001m	0.0006m

In demonstrating and investigation of the cantilevered beam, following suppositions are considered: -

- a) The beam, PZT patch/patches are taken as Euler-Bernoulli beam elements i.e. effect of transverse shear forces is disposed.
- b) PZT patch/patches is/are thin related with the beam thickness.
- c) Cross-segments regions of beam, PZT patch/patches remain plane and normal to the deformed longitudinal axis before and also after bending.
- d) Neutral axis of beam, PZT patch/patches pass through their centroid.
- e) The polarization direction of the PZT patch/patches is in the thickness direction (z-axis)
- f) The piezoelectric material is identical, transverse isotropic and flexible.
- g) Adhesive utilised in holding the PZT patch/patches does not contribute in mass and stiffness of Smart beam element.

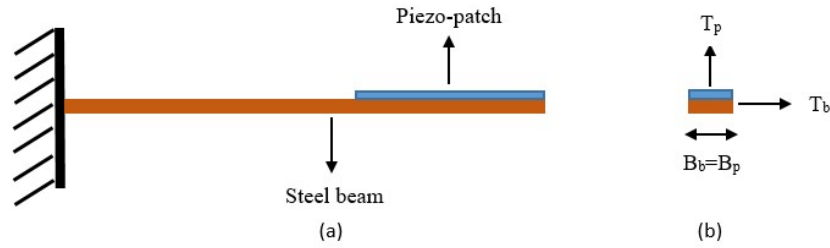


**Figure 3.2 (a) cantilevered beam with piezoelectric material (b) cross-section of beam**

In the present study suffix ‘*b*’ is used for cantilevered beam element, suffix ‘*p*’ is used for PZT patch layer as shown in Figure 3.2.  $A_b$  and  $A_p$  are cross-sectional areas of cantilevered beam and PZT patch layers respectively.  $I_b$  and  $I_p$  are moment of Inertias of cantilevered beam and PZT patch layers respectively.  $T_b$  and  $T_p$  are thickness of cantilevered beam and piezo-patch material.  $B_b$  and  $B_p$  are width of regular beam and piezo-patch material.

### 3.3.2 Mathematical Modelling of Regular Beam

The beam with a patch has non uniform cross section along the length and needs to be modelled as variable cross section beam. However, initially a uniform cross section beam is modelled and analysed before the analysis of variable cross section beam. Figure 3.3 shows the model of a cantilevered beam of length  $L$ . The Euler-Bernoulli beam theory, for a beam is given by

$$EI \frac{\partial^4 w}{\partial x^4} + \rho A \frac{\partial^2 w}{\partial t^2} = f(t)$$

where  $EI$  is the flexural unbending of the beam,  $\rho$  is the density of the beam,  $A$  is the cross section area of the beam,  $x$  is the longitudinal facilitate,  $w$  is the transverse motion of the beam,  $t$  is the time,  $f(t)$  is the outer force vector.



**Figure 3.3 Cantilevered beam**

### 3.3.2.1 The Solution Procedure (Modal Superposition Method)

In this section, for calculating the dynamic response of the cantilevered beam a modal superposition method is adopted.

This method is built up on the dynamic response of cantilevered beam can be approximated utilizing the stacked superposition of some undamped linear modes of the un-diverted beam structure. Accordingly, the movement of the cantilevered beam  $w(x, \tau)$  is explained in a variable separable form as: -

$$w(x, \tau) = \sum_{j=1}^N \phi_j(x) \eta_j(\tau) \quad (3.1)$$

in which  $\phi_i(x)$  represents the  $i^{th}$  mode shape of the un deformed beam,  $\eta_i(\tau)$  is the modal coordinate, and N denotes the total number of modes. In the present study cantilevered beam is taken as test model and boundary conditions of cantilevered beam are as follows.

$$w|_{x=0} = 0 \quad \frac{\partial w}{\partial x}|_{x=0} = 0 \quad \frac{\partial^2 w}{\partial x^2}|_{x=l} = 0 \quad \frac{\partial^3 w}{\partial x^3}|_{x=l} = 0 \quad (3.2)$$

By using above boundary conditions and applying modal superposition method on Euler-Bernoulli governing equation which is composed as

$$\sum_{i=1}^N \phi_i''' \eta_k + \sum_{i=1}^N \phi_i \ddot{\eta}_k = 0 \quad (3.3)$$

Multiplying with  $\phi_k$  and integrate the equation over the domain i.e. 0 to length of the beam( $l$ ). following equation becomes.

$$\int_0^l \sum_{i=1}^N \phi_i''' \phi_k \eta_k + \int_0^l \sum_{i=1}^N \phi_i \phi_k \ddot{\eta}_k = 0 \quad (3.4)$$

By adopting the principle of orthogonality equation reduces the governing differential equation to a set of N coupled second order ordinary differential equations which is written as

$$[M] (\eta_k) + [K](\eta_k) = F \quad (3.5)$$

where M and K represent the mass and the stiffness matrix, individually, and the vector F depicts the vector of generalized modal forces. Instead of using flow excitation an external

harmonic sinusoidal force  $F$  is acting at the specific node of the cantilevered beam in unimorph configuration as shown in Figure 3.4.

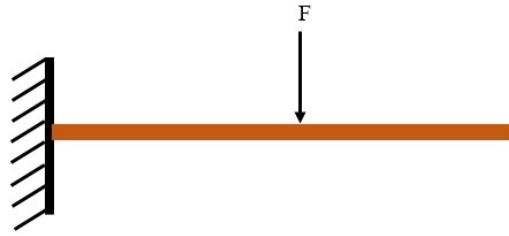


**Figure 3.4 Sinusoidal force acting on cantilevered beam**

For calculating the dynamic response of a cantilevered beam, these equations are integrated using the ODE solver available in MATLAB.

### 3.2.3 Dynamic Response of Cantilever Stepped Beam

In the previous section, mathematical modelling of the regular cantilevered beam is discussed. In this section, the mathematical modelling of the stepped beam as shown in Figure 3.5 is done. When the piezoelectric material patch is attached on the cantilevered beam then it becomes the beam of variable thickness. therefore, for investigating the dynamic response of a cantilevered beam with variable or non-uniform thickness the methodology of vibration in stepped beam is considered.

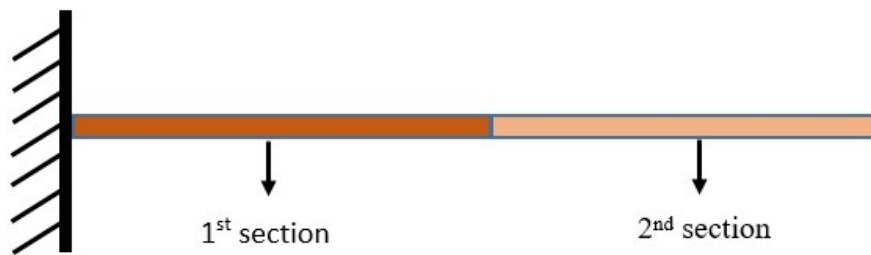


**Figure 3.5 cantilevered beam with two sections**

The governing differential equation for the small amplitude, free, lateral vibration of a Bernoulli-Euler beam is

$$EI \frac{\partial^4 w}{\partial x^4} + \rho A \frac{\partial^2 w}{\partial t^2} = f(t) \quad (3.6)$$

where  $A$  is the cross-sectional area,  $EI$  the flexural unbending,  $t$  is the time,  $x$  the position along the beam,  $w$  the beam motions, and  $\rho$  is the density of material. Presuming normal modes, with frequency  $w$ , one obtains the following expression for the mode shape  $X$ :

$$\frac{\partial^2}{\partial x^2} (EI(x) \frac{\partial^2 X}{\partial x^2}) = w^2 \rho A(x) X \quad (3.7)$$

For a stepped beam (see Figure 3.5), one can rewrite Equation (3.7) as

$$\frac{\partial^4 X_i}{\partial x_i^4} = K_i^4 X_i \quad (3.8)$$

Where  $K_i^4 = (\rho A_i / EI_i) w^2$  and  $i=1,2$

The common solution of equation is

$$X_1 = C_1 \sin K_1 x_1 + C_2 \cos K_1 x_1 + C_3 \sin K_1 x_1 + C_4 \cosh K_1 x_1,$$

$$X_2 = C_5 \sin K_2 x_2 + C_6 \cos K_2 x_2 + C_7 \sin K_2 x_2 + C_8 \cosh K_2 x_2, \quad (3.8)$$

In the present study, cantilevered beam i.e. fixed free beam is used as a test model. In this section cantilevered beam is divide into two sections as shown in Figure 3.5 and the boundary conditions at the fixed and free end is written as

$$w|_{x=0} = 0 \quad \frac{\partial w}{\partial x}|_{x=0} = 0 \quad \frac{\partial^2 w}{\partial x^2}|_{x=l_2} = 0 \quad \frac{\partial^3 w}{\partial x^3}|_{x=l_2} = 0 \quad (3.9)$$

Stress focus at the intersection of the two sections of the beam is disregarded. Then, at that point, at the intersection, the continuity of deflection, slope, moment and shear force has to be preserved. Thus,

$$X_1(L_1) = X_2(L_2), \quad \frac{dX_1}{dx_1}(L_1) = \frac{dX_2}{dx_2}(L_2), \quad I_1 \frac{d^2 X_1}{dx_1^2}(L_1) = I_2 \frac{d^2 X_2}{dx_2^2}(L_2),$$

$$\frac{d}{dx_1} \left( I_1 \frac{d^2 X_1}{dx_1^2} \right) (L_1) = \frac{d}{dx_2} \left( I_2 \frac{d^2 X_2}{dx_2^2} \right) (L_2) \quad (3.10)$$

The formulation of the fixed free beam problem is as follows. Equations (3.9) and (3.10)

$C_3 = -C_1$ ,  $C_4 = -C_2$  Also, let

$$S1 = \sin K_1 L_1, \quad S2 = \sin K_2 L_2, \quad C1 = \cos K_1 L_1, \quad C2 = \cos K_2 L_2,$$

$$SH1 = \sinh K_1 L_1, \quad SH2 = \sinh K_2 L_2, \quad CH1 = \cosh K_1 L_1, \quad CH2 = \cosh K_2 L_2$$

$$K = \frac{K_2}{K_1}, \quad I = \frac{I_2}{I_1} \quad (3.11)$$

Then Equation (3.8) yield the following set of equations:

$$\begin{bmatrix} 0 & 0 & -S2 & -C2 & SH2 & CH2 \\ 0 & 0 & -C2 & S2 & CH2 & SH2 \\ S1-SH1 & C1-CH1 & 0 & 1 & 0 & 1 \\ C1-CH1 & -S1-SH1 & K & 0 & K & 0 \\ -S1-SH1 & -C1-CH1 & 0 & -I*K^2 & 0 & I*K^2 \\ -C1-CH1 & S1-SH1 & -I*K^3 & 0 & I*K^3 & 0 \end{bmatrix} \begin{Bmatrix} c1 \\ c2 \\ c5 \\ c6 \\ c7 \\ c8 \end{Bmatrix} = 0 \quad (3.12)$$

From the above matrix unknowns are calculated by using the gauss elimination method. By putting the values of unknowns in general Equation (3.8) the two mode shape equations of both the sections are obtained. The combined mode equation of both the section of beam is obtained by applying Heaviside function methodology. Hence the whole methodology of mathematical modelling of regular beam is repeated on the beam of two sections therefore, the dynamic response of cantilevered beam of two section is calculated.

### 3.2.4 Dynamic Response of Cantilevered Stepped Beam of Three Sections

In this section, the dynamic response of cantilevered beam of three section as shown in Figure 3.6 is calculated. In the same manner the whole methodology is also repeated for dynamic response of three section beam.

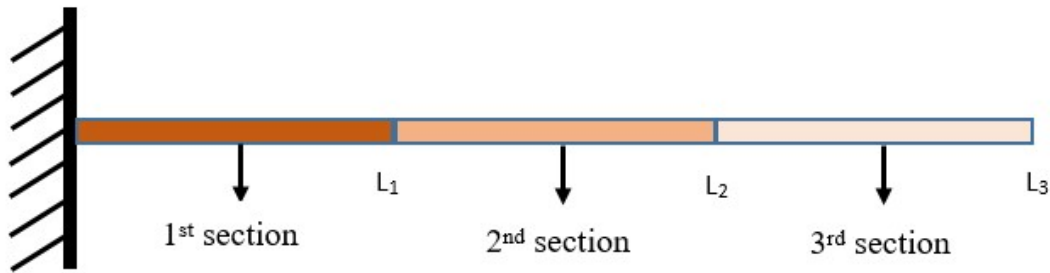


**Figure 3.6 cantilevered beam of three sections**

The general mode shape equation for cantilevered beam of three sections is written as

$$\begin{aligned} X_1 &= C_1 \sin K_1 X_1 + C_2 \cos K_1 X_1 + C_3 \sin K_1 X_1 + C_4 \cosh K_1 X_1, \\ X_2 &= C_5 \sin K_2 X_2 + C_6 \cos K_2 X_2 + C_7 \sin K_2 X_2 + C_8 \cosh K_2 X_2, \\ X_2 &= C_9 \sin K_3 X_3 + C_{10} \cos K_3 X_3 + C_{11} \sin K_3 X_3 + C_{12} \cosh K_3 X_3, \end{aligned} \quad (3.13)$$

In the present study, cantilevered beam i.e. fixed free beam is used as a test model. In this section cantilevered beam is divide into three sections as shown in Figure 3.6 and the boundary conditions at the fixed and free end is written as

$$w|_{x=0} = 0 \quad \frac{\partial w}{\partial x}|_{x=0} = 0 \quad \frac{\partial^2 w}{\partial x^2}|_{x=l_3} = 0 \quad \frac{\partial^3 w}{\partial x^3}|_{x=l_3} = 0 \quad (3.14)$$

In this section cantilevered beam consist of three sections therefore, there are two junction Stress concentration at the two junctions of the three parts of the beam is neglected. Then, at the junctions, the continuity of deflection, slope, moment and shear force has to be preserved.

Thus, For junction 1,

$$\begin{aligned} X_1(L_1) &= X_2(L_2), & \frac{dX_1}{dx_1}(L_1) &= \frac{dX_2}{dx_2}(L_2), & I_1 \frac{d^2 X_1}{dx_1^2}(L_1) &= I_2 \frac{d^2 X_2}{dx_2^2}(L_2), \\ \frac{d}{dx_1} \left( I_1 \frac{d^2 X_1}{dx_1^2} \right) (L_1) &= \frac{d}{dx_2} \left( I_2 \frac{d^2 X_2}{dx_2^2} \right) (L_2) \end{aligned} \quad (3.15)$$

For junction 2,

$$\begin{aligned} X_2(L_2) &= X_3(L_3), & \frac{dX_2}{dx_2}(L_2) &= \frac{dX_3}{dx_3}(L_3), & I_2 \frac{d^2 X_2}{dx_2^2}(L_2) &= I_3 \frac{d^2 X_3}{dx_3^2}(L_3), \\ \frac{d}{dx_2} \left( I_2 \frac{d^2 X_2}{dx_2^2} \right) (L_2) &= \frac{d}{dx_3} \left( I_3 \frac{d^2 X_3}{dx_3^2} \right) (L_3) \end{aligned} \quad (3.16)$$

The formulation of the fixed free beam problem is as follows, Equations (3.15) and (3.16)

$C_3 = -C_1$ ,  $C_4 = -C_2$  Also, let

$$\begin{aligned} S1 &= \sin K_1 L_1, & S2 &= \sin K_2 L_2, & C1 &= \cos K_1 L_1, & C2 &= \cos K_2 L_2, \\ SH1 &= \sinh K_1 L_1, & SH2 &= \sinh K_2 L_2, & CH1 &= \cosh K_1 L_1, & CH2 &= \cosh K_2 L_2, \\ S3 &= \sin K_3 L_3, & C3 &= \cos K_3 L_3, & SH3 &= \sinh K_3 L_3, & CH3 &= \cosh K_3 L_3, \end{aligned}$$

$$K_1 = \frac{K_2}{K_1}, \quad I_1 = \frac{I_2}{I_1}, \quad K_2 = \frac{K_3}{K_2}, \quad I_2 = \frac{I_3}{I_2} \quad (3.17)$$

Then Equation (3.13) yield the following set of equations:

$$\begin{bmatrix}
 S1 - SH1 & C1 - CH1 & 0 & 1 & 0 & 1 & 0 & 0 & 0 & 0 \\
 C1 - CH1 & -S1 - SH1 & KK & 0 & KK & 0 & 0 & 0 & 0 & 0 \\
 -S1 - SH1 & -C1 - CH1 & 0 & -II * KK^2 & 0 & I * KK^2 & 0 & 0 & 0 & 0 \\
 -C1 - CH1 & S1 - SH1 & -II * KK^3 & 0 & II * KK^3 & 0 & 0 & 0 & 0 & 0 \\
 0 & 0 & S2 & C2 & SH2 & CH2 & 0 & 1 & 0 & 1 \\
 0 & 0 & C2 & -S2 & CH2 & SH2 & KK2 & 0 & KK2 & 0 \\
 0 & 0 & -S2 & -C2 & SH2 & CH2 & 0 & -II2 * KK2^2 & 0 & II2 * KK2^2 \\
 0 & 0 & -C2 & S2 & CH2 & SH2 & -II2 * KK2^2 & 0 & II2 * KK2^2 & 0 \\
 0 & 0 & 0 & 0 & 0 & 0 & -S3 & -C3 & SH3 & CH3 \\
 0 & 0 & 0 & 0 & 0 & 0 & -C3 & S3 & CH3 & SH3
 \end{bmatrix}
 \begin{Bmatrix}
 C_1 \\
 C_2 \\
 C_5 \\
 C_6 \\
 C_7 \\
 C_8 \\
 C_9 \\
 C_{10} \\
 C_{11} \\
 C_{12}
 \end{Bmatrix}
 = 0$$

From the above matrix unknowns are calculated by using the gauss elimination method. By putting the values of unknowns in general Equation (3.13) the three mode shape equations of three sections are obtained. The combined mode equation of both the section of beam is obtained by applying Heaviside function methodology. Hence the whole methodology of mathematical modelling of regular beam is repeated on the beam of three sections therefore, the dynamic response of cantilevered beam of three section is calculated.

### 3.2.5 Estimating The Charge Generation from Cantilevered Beam with Piezoelectric Material Patch.

In this section, estimating of the charge generation from the deflection of the cantilevered beam along with piezoelectric material patch is discussed.

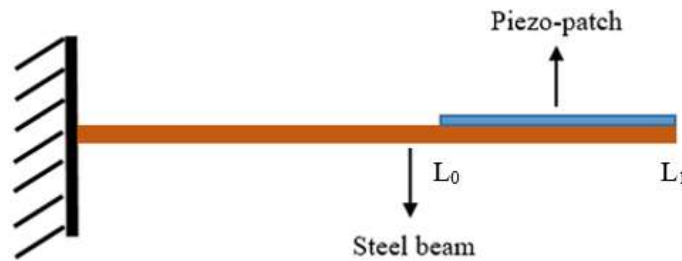


**Figure 3.7 cantilevered beam with piezoelectric material patch**

First of all, when beam undergo deflection mechanism the following strain is generated along the beam with the compression and expansion of the piezoelectric material patch therefore, charge is generated. This is also called piezoelectric effect. The direct piezoelectric effect is implemented to estimate the output charge on the PZT layer originated by the strains in the beam. The strain in the direction of x-coordinate as

$$\varepsilon_x = -z \frac{\partial^2 w}{\partial x^2} \quad (3.18)$$

Where  $w$  is the transverse deflection of the beam and  $z$  is the distance from the neutral plane.

The linear piezoelectric theory is adopted. The charge in the x-bearing is dared to be zero,  $D_x = 0$ . The worry in the z-heading is ventured to be zero inside the piezoelectric fix,  $\sigma_z |z| = 0$ . This assumption is authoritative when the piezoelectric layer thickness in comparison

to the length of the beam is very thin. Following Linear Piezoelectric Constitutive Equation (3.19) will be used for deriving the PZT equation.

$$D_z = e_{31}\varepsilon_x + \epsilon_{33} E_z \quad (3.19)$$

Where  $\varepsilon_x$  is Stress,  $e_{31}$  is Piezoelectric Constant (Coulomb/N or m/V),  $E_z$  is Electric field (Volt/m),  $D_z$  is Electric displacement i.e. charge per unit area (Coulomb/m<sup>2</sup>),  $\epsilon_{33}$  is Dielectric constant (Permittivity) under uniform stress. The direct piezoelectric impact is utilized to evaluate the yield charge on the PZT layer made by the strains in the beam. Since no electric field is applied to the PZT layer. The above equation is written as.

$$D_z = e_{31}\varepsilon_x \quad (3.20)$$

The charge gathered on the terminal surface can be represents as the electrical displacement integral on the area of the surface is written as.

$$Q = \int_A D_z dA = b \int_{l_0}^{l_1} (e_{31}\varepsilon_x) dx \quad (3.21)$$

Where  $b$  is the width of the beam (assumed to be constant along the whole range) and  $L_0$  to  $L_1$  is the length limits of the piezoelectric material patch as shown in Figure 3.7 above.

### 3.4 Validation of Methodology

In this section, the testing of the methodology has been done. The developed solution method has been validated with the standard results available in the literature[Rao.]. A simply supported beam is excited for a harmonic point force of amplitude and frequency at 1/3 from one end. The dynamic response of simply supported beam is calculated by the following formula is written as:

$$w(x, t) = \frac{2f_0}{\rho Al} \sum_{n=1}^{\infty} \frac{1}{w_n^2 - w^2} \sin \frac{n\pi a}{l} \sin \frac{n\pi x}{l} \sin wt$$

Where  $l$  is the length of beam,  $A$  is area of cross-section,  $\rho$  is the density of material,  $f_0$  is force applied on beam,  $w$  is frequency given to beam and  $w_n$  is natural frequency of the beam.

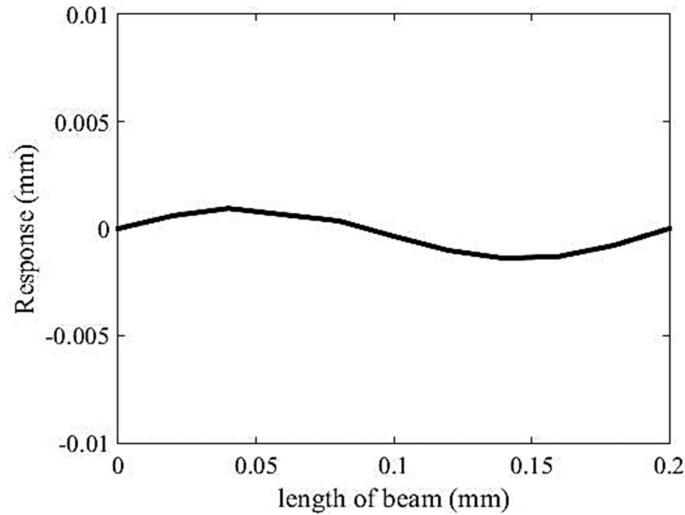


**Figure 3.8 Response of simply supported beam with analytical solution. [Rao]**

Figure 3.8 shows the response of the beam obtained from the analytical solution [Rao.]. The developed methodology discussed in this chapter has been also applied on the simply supported beam. Figure 3.9 shows the response of the simply supported beam when the beam is excited for a harmonic point force of amplitude and frequency at 1/3 from one end.

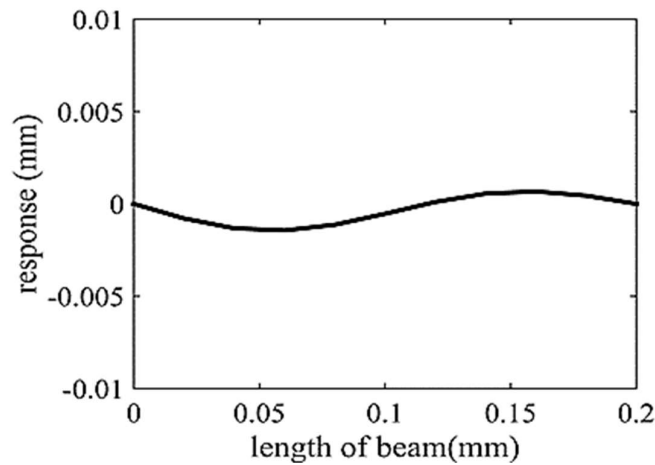


**Figure 3.9 Response of beam with present methodology**

The results obtain from both formulation depicts the same value of response of the developed model as shown in Figures 3.8 and 3.9. Hence The validated model is employed for calculation of electric charge from a piezoelectric cantilevered patches. Different harmonic excitation such as single/multiple frequency excitation has been employed and results are ongoing.

## Summary

In this section, the Methodology for analysis of energy harvesting from a cantilevered beam with piezoelectric layer have been discussed. Firstly, the Euler-Bernoulli beam theory is adopted and mathematical modelling of the beam is done by using modal superposition method. Initially, dynamic response of the regular beam is calculated. Then for modelling of piezoelectric material patch with beam, a stepped beam model is considered. The direct piezoelectric effect is used to calculate the output charge on the PZT layer created by the strains in the beam.

# CHAPTER 4

## RESULTS AND DISCUSSION

---

In this chapter, the methodology, discussed in the previous chapter, is implemented to estimate the charge generation from the deflection of cantilevered beam with piezoelectric material patch. The optimal position of the piezoelectric patch material where maximum charge generation takes place is also investigated.

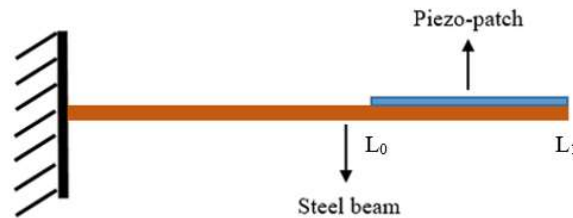


Figure 4.1 cantilevered beam with piezoelectric patch

Figure 4.1 shows a cantilevered beam with piezoelectric patch. The equivalent mathematical model of beam with patch is shown in Figure 4.2. It may be noted that in the mathematical model, a three section beam is considered, which will allow analysing the system for different position of the patch.

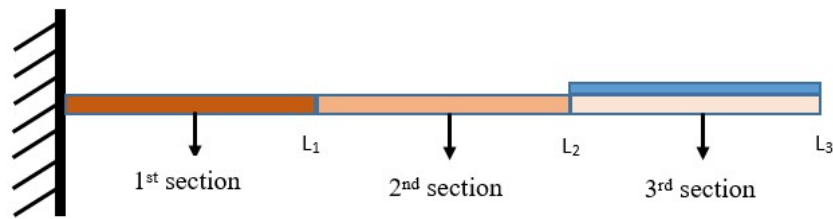


Figure 4.2 cantilevered stepped beam

Table 4.1 Shows the property of beam and PZT patch used for the analysis.

Specifications	Test models	
	Beam	PZT-Patch
Young's modulus	210GPa	63GPa
Density	7800 Kg/m <sup>3</sup>	7500 Kg/m <sup>3</sup>
Length	0.3m	0.1m

<b>Width</b>	0.03m	0.03m
<b>Thickness</b>	0.001m	0.0006m

Piezoelectric patch is attached on the beam. Instead of using flow excitation an external harmonic sinusoidal force  $F$  is acting at the specific node of the cantilevered beam in unimorph configuration. Analytically the three natural frequency of the smart beam is calculated by the following formula.

$$w = \beta^2 \sqrt{\frac{EI}{\rho A}}$$

Figure 4.3(a)-(c) shows the natural modes of the beam and corresponding three natural frequencies of the equivalent beam are shown in Table 4.2

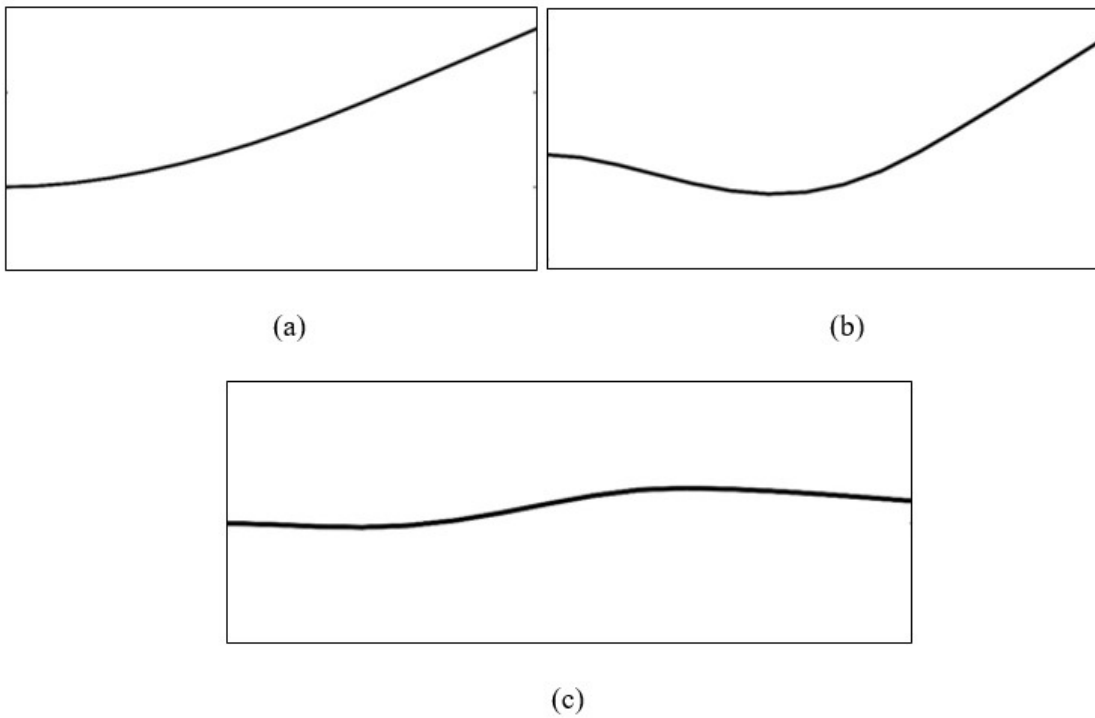


**Figure 4.3 (a)-(c) Natural modes of the beam**

**Table 4.2 Corresponding three natural frequencies of the equivalent beam**

<b>Sr.No</b>	<b>Natural frequency ( Hz)</b>
1 <sup>st</sup>	7.8632
2 <sup>nd</sup>	60.9828
3 <sup>rd</sup>	185.6167

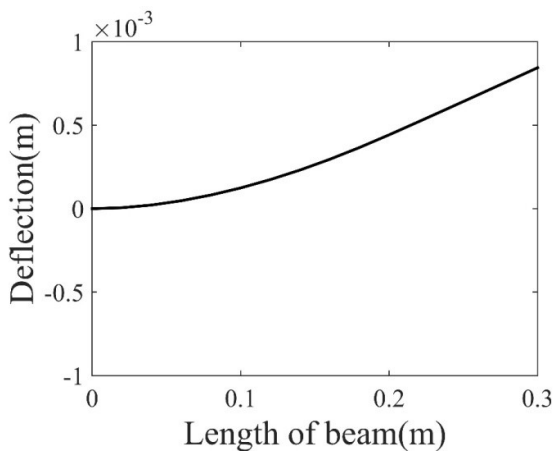
In case of the piezoelectric material patch is associated at the tip of the beam, the properties of the combined section will be different from the rest of the beam. As in the present model, the cantilevered beam consists of three sections, as shown in Figure 4.2, among these, the 3<sup>rd</sup> section of the beam is combined section. The properties of first two sections of the beam and the 3<sup>rd</sup> section which is combined with piezoelectric material patch are shown in Table 4.3

**Table 4.3 Properties of different section in cantilevered beam**

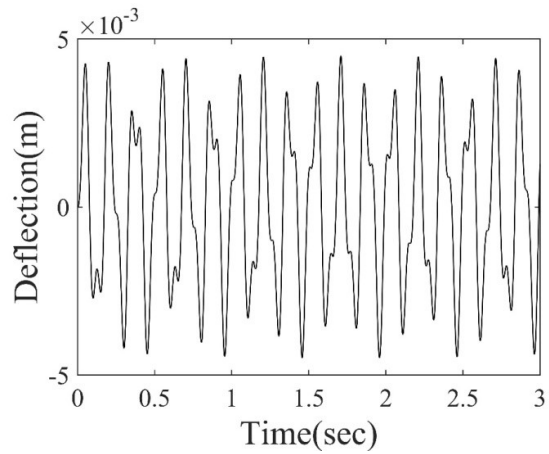
Properties	Sections of the cantilevered beam	
	1 <sup>st</sup> and 2 <sup>nd</sup> section	3 <sup>rd</sup> section
Young's modulus of elasticity (E)	210GPa	273GPa
Density of material	7800 Kg/m <sup>3</sup>	7650 Kg/m <sup>3</sup>

#### 4.1 Response of the Beam

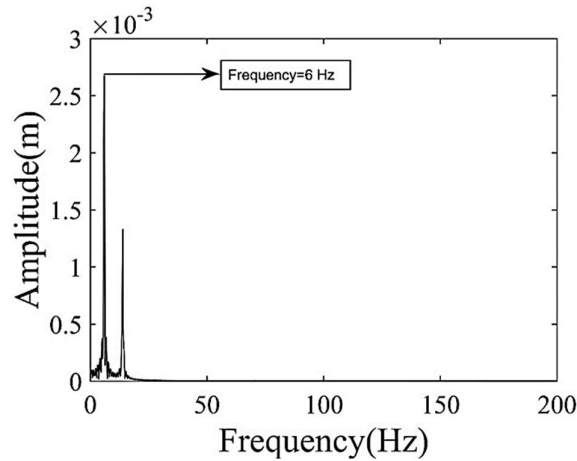
To get the response of the beam, the beam is excited at a point 0.25 away from the fixed end. For the excitation, different excitation frequencies are considered. Figure 4.4 (a)-(c) shows the mode shape, time history and frequency spectrum of the beam vibration for an excitation of  $F=A \sin (2\pi*6*t)$ . where A is the excitation amplitude and the beam is excited at 6 Hz frequency. The figure indicates that the deflection shape of the beam is close to the first bending mode of the beam, which is expected as the excitation frequency is close to the first natural frequency. The frequency spectrum indicates two peaks corresponding to 6 Hz and 7.86 Hz which are corresponding to excitation and first modal frequency.



(a)



(b)

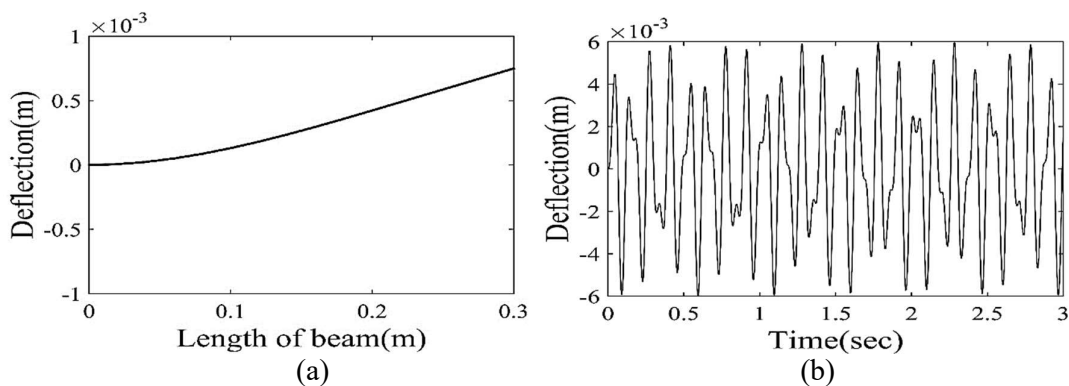


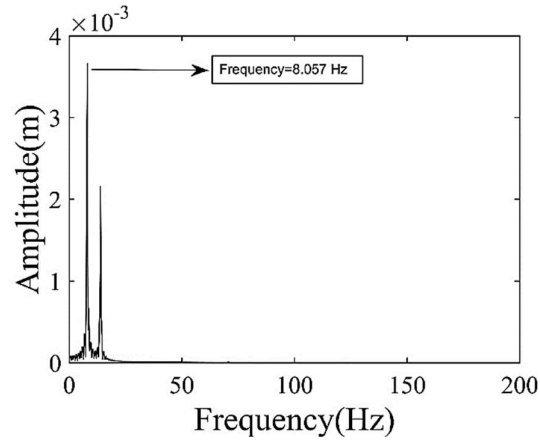
(c)

**Figure 4.4 (a)Mode of vibration (b)Time response graph (c) frequency spectrum**

The dynamic response of cantilevered beam is calculated by giving the excitation frequency of 6 Hz nearly the first natural frequency of the beam calculated above as shown in Table 4.2. The cantilevered beam is entirely excited in first mode of vibration. In Figure 4.4(a) the mode shape of the beam is shown. The time response at the tip of the cantilevered beam is investigated shown in Figure 4.4(b). Frequency spectrum of the time response signal at the tip of the beam is also obtained shown in Figure 4.4(c). from the above figures it is seen that the cantilevered beam is entirely vibrates in the first mode of vibration by giving the frequency of 6 Hz.

Figure 4.5(a)-(c) shows the mode shape, time history and frequency spectrum of the beam vibration for an excitation of  $F=A \sin (2\pi*8t)$ . where A is the excitation amplitude and the beam is excited at 8 Hz frequency. The figure indicates that the deflection shape of the beam is close to the first bending mode of the beam, which is expected as the excitation frequency is close to the first natural frequency. The frequency spectrum indicates two peaks corresponding to 8 Hz and 7.86 Hz which are corresponding to excitation and first modal frequency.



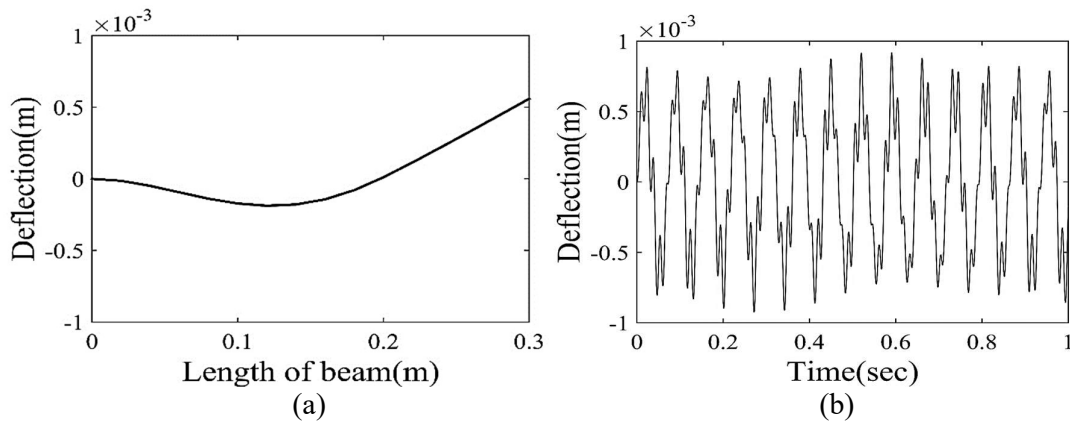


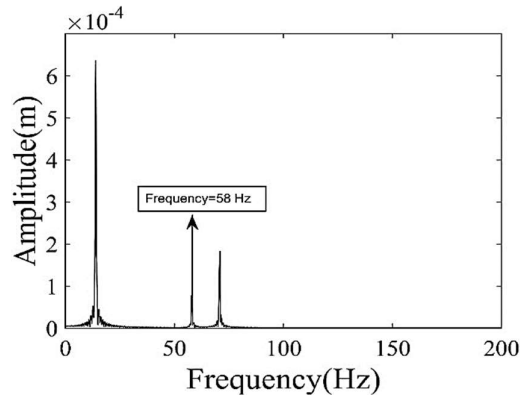
(c)

**Figure 4.5 (a)Mode of vibration (b)Time response graph (c) frequency spectrum**

The dynamic response of cantilevered beam is calculated by giving the excitation frequency of 8 Hz nearly the first natural frequency of the beam calculated above as shown in Table 4.2. The cantilevered beam is entirely excited in first mode of vibration. In Figure 4.5(a) the mode shape of the beam is shown. The time response at the tip of the cantilevered beam is investigated shown in Figure 4.5(b). Frequency spectrum of the time response signal at the tip of the beam is also obtained shown in Figure 4.5(c). from the above figures it is seen that the cantilevered beam is entirely vibrates in the first mode of vibration by giving the frequency of 8 Hz.

Figure 4.6(a)-(c) shows the mode shape, time history and frequency spectrum of the beam vibration for an excitation of  $F=A \sin (2\pi*58t)$ . where A is the excitation amplitude and the beam is excited at 58 Hz frequency. The figure indicates that the deflection shape of the beam is close to the first bending mode of the beam, which is expected as the excitation frequency is close to the first natural frequency. The frequency spectrum indicates three peaks corresponding to 58 Hz, 7.86 Hz and 60.98 Hz which are corresponding to excitation, first and second modal frequency.



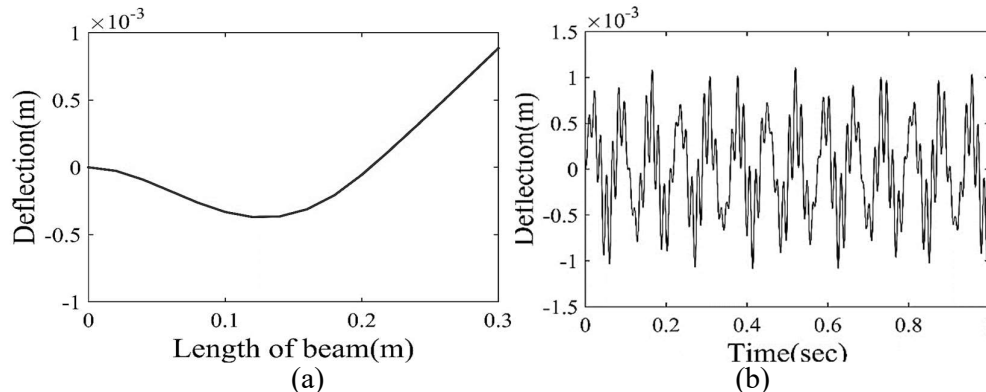


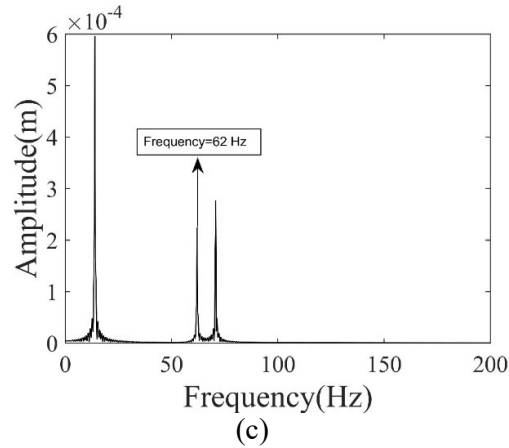
(c)

**Figure 4.6 (a)Mode of vibration (b)Time response graph (c) frequency spectrum**

The dynamic response of cantilevered beam is calculated by giving the excitation frequency of 58 Hz nearly the second natural frequency of the beam calculated above as shown in Table 4.2. The cantilevered beam is entirely excited in second mode of vibration. In Figure 4.6(a) the mode shape of the beam is shown. The time response at the tip of the cantilevered beam is investigated shown in Figure 4.6(b). Frequency spectrum of the time response signal at the tip of the beam is also obtained shown in Figure 4.6(c). from the above figures it is seen that the cantilevered beam is entirely vibrates in the second mode of vibration by giving the frequency of 58 Hz.

Figure 4.7(a)-(c) shows the mode shape, time history and frequency spectrum of the beam vibration for an excitation of  $F=A \sin (2\pi*62t)$ . where A is the excitation amplitude and the beam is excited at 58 Hz frequency. The figure indicates that the deflection shape of the beam is close to the first bending mode of the beam, which is expected as the excitation frequency is close to the first natural frequency. The frequency spectrum indicates three peaks corresponding to 62 Hz, 7.86 Hz and 60.98 Hz which are corresponding to excitation, first and second modal frequency.

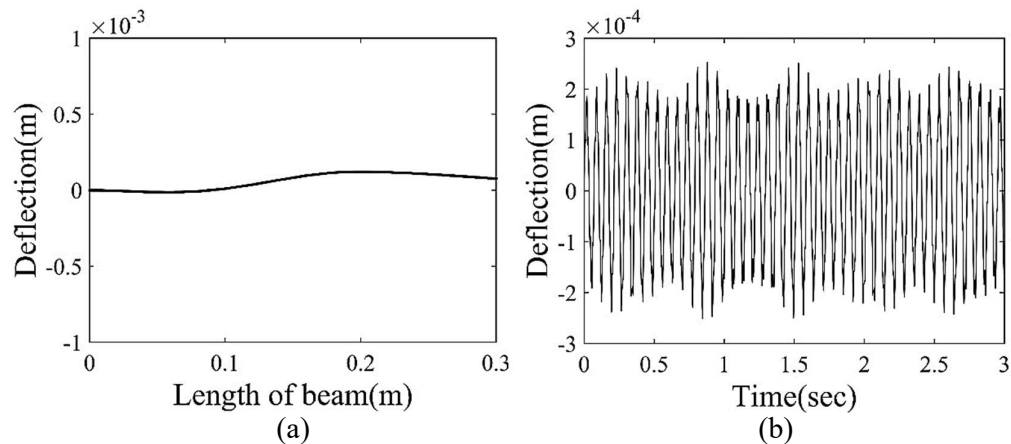


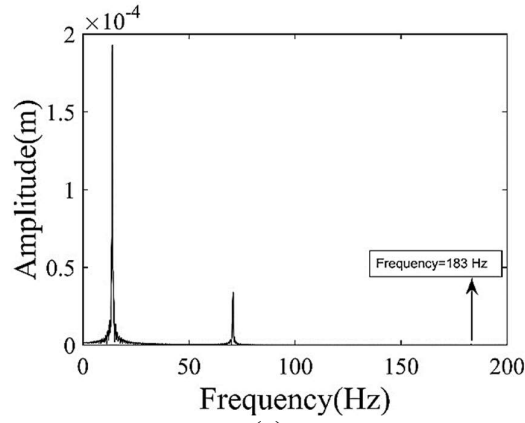


**Figure 4.7 (a)Mode of vibration (b)Time response graph (c) frequency spectrum**

The dynamic response of cantilevered beam is calculated by giving the excitation frequency of 62 Hz nearly the second natural frequency of the beam calculated above as shown in Table 4.2. The cantilevered beam is entirely excited in second mode of vibration. In Figure 4.7(a) the mode shape of the beam is shown. The time response at the tip of the cantilevered beam is investigated shown in Figure 4.7(b). Frequency spectrum of the time response signal at the tip of the beam is also obtained shown in Figure 4.7(c). from the above figures it is seen that the cantilevered beam is entirely vibrates in the second mode of vibration by giving the frequency of 62 Hz.

Figure 4.8(a)-(c) shows the mode shape, time history and frequency spectrum of the beam vibration for an excitation of  $F=A \sin (2\pi*183t)$ . where A is the excitation amplitude and the beam is excited at 183 Hz frequency. The figure indicates that the deflection shape of the beam is close to the third bending mode of the beam, which is expected as the excitation frequency is close to the third natural frequency. The frequency spectrum indicates three peaks corresponding to 183 Hz, 7.86 Hz and 60.98 Hz which are corresponding to excitation, first and second modal frequency.



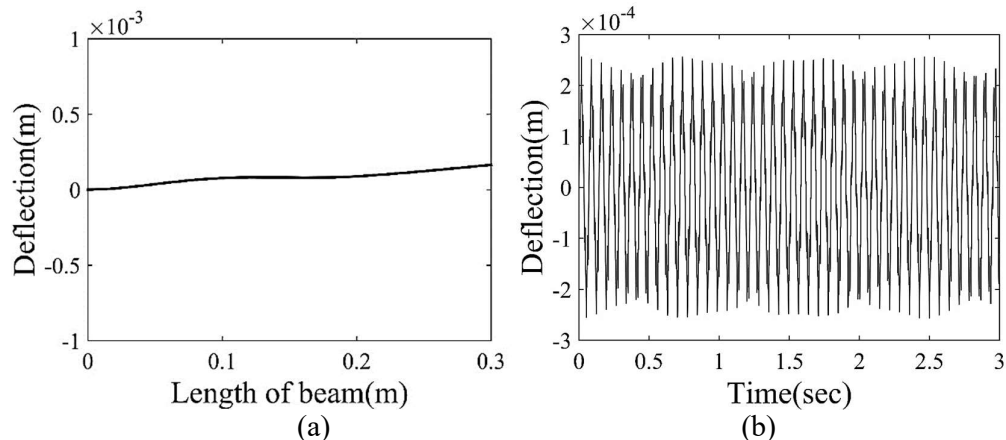


(c)

**Figure 4.8 (a) Mode of vibration (b) Time response graph (c) frequency spectrum**

The dynamic response of cantilevered beam is calculated by giving the excitation frequency of 183 Hz nearly the third natural frequency of the beam calculated above as shown in Table 4.2. The cantilevered beam is entirely excited in third mode of vibration. In Figure 4.8(a) the mode shape of the beam is shown. The time response at the tip of the cantilevered beam is investigated shown in Figure 4.8(b). Frequency spectrum of the time response signal at the tip of the beam is also obtained shown in Figure 4.8(c). From the above figures it is seen that the cantilevered beam is entirely vibrates in the third mode of vibration by giving the frequency of 183 Hz.

Figure 4.9(a)-(c) shows the mode shape, time history and frequency spectrum of the beam vibration for an excitation of  $F=A \sin(2\pi \cdot 186t)$ , where  $A$  is the excitation amplitude and the beam is excited at 186 Hz frequency. The figure indicates that the deflection shape of the beam is close to the third bending mode of the beam, which is expected as the excitation frequency is close to the third natural frequency. The frequency spectrum indicates three peaks corresponding to 186 Hz, 7.86 Hz and 60.98 Hz which are corresponding to excitation, first and second modal frequency.



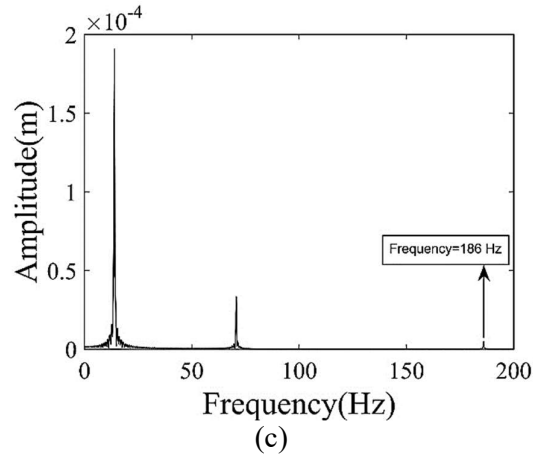
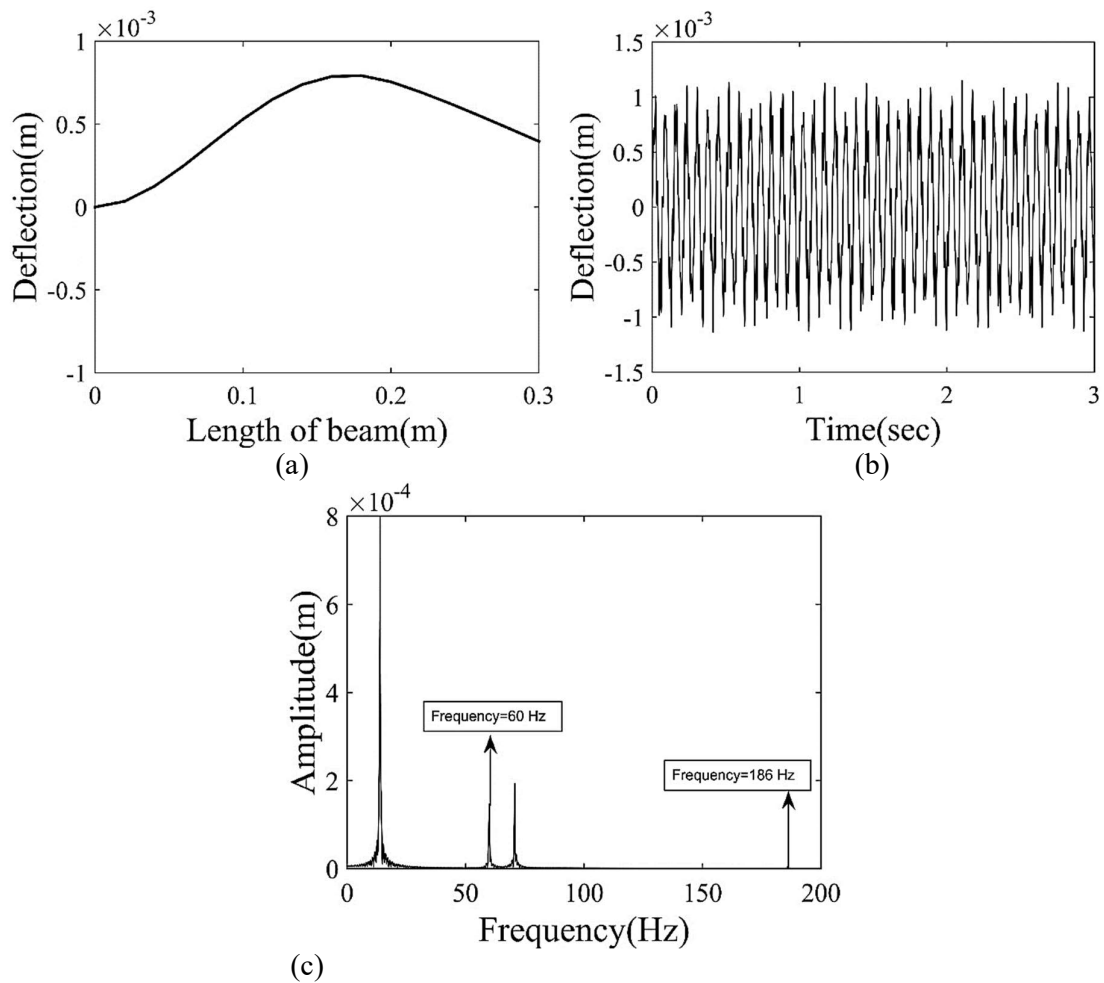


**Figure 4.9 (a) Mode of vibration (b) Time response graph (c) frequency spectrum**

The dynamic response of cantilevered beam is calculated by giving the excitation frequency of 186 Hz nearly the third natural frequency of the beam calculated above as shown in Table 4.2. The cantilevered beam is entirely excited in third mode of vibration. In Figure 4.9(a) the mode shape of the beam is shown. The time response at the tip of the cantilevered beam is investigated shown in Figure 4.9(b). Frequency spectrum of the time response signal at the tip of the beam is also obtained shown in Figure 4.9(c). From the above figures it is seen that the cantilevered beam is entirely vibrates in the third mode of vibration by giving the frequency of 186 Hz.

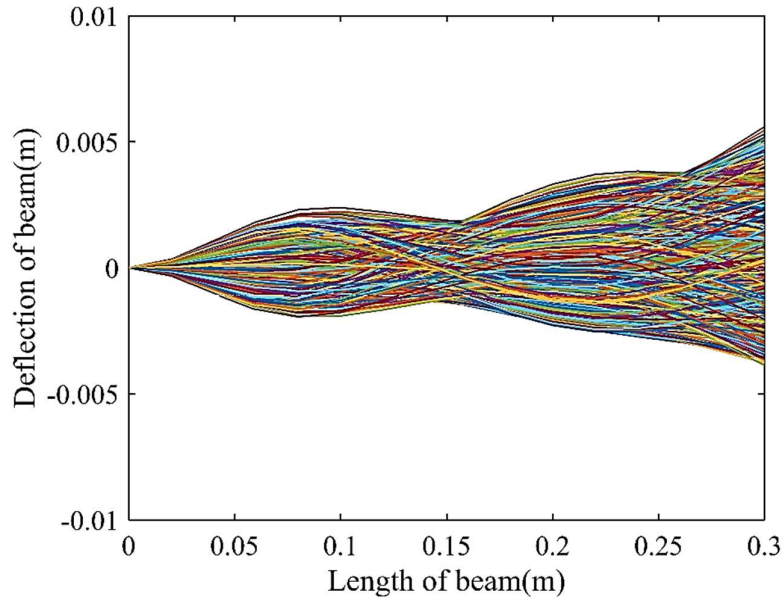
As we seen above so far response of beam corresponding to single excitation frequency. It has been noted in the investigation that response of the cantilevered beam has been checked for the different excitation frequency close to the natural modal frequency of cantilevered beam. However, in case of flow induced vibration it is noted that the response of the vibration of cantilevered beam is multiple mode of vibration undergoes simultaneously. Therefore, to simulate that effect in the beam it has been excited with the multiple frequencies. For that purpose, three natural frequencies are considered as shown in Table 4.1.

Figure 4.10(a)-(c) shows the mode shape, time history and frequency spectrum of the beam vibration for an excitation of  $F = A \sin(2\pi \cdot 60t) + A \sin(2\pi \cdot 186t)$ . where  $A$  is the excitation amplitude and the beam is excited at two modal natural frequencies i.e. 60 Hz and 186 Hz frequency. The figure indicates that the deflection shape of the beam is close to the mix bending mode of the beam. The frequency spectrum indicates two peaks corresponding to 186 Hz and 60.98 Hz which are corresponding to excitation, second and third modal frequency.



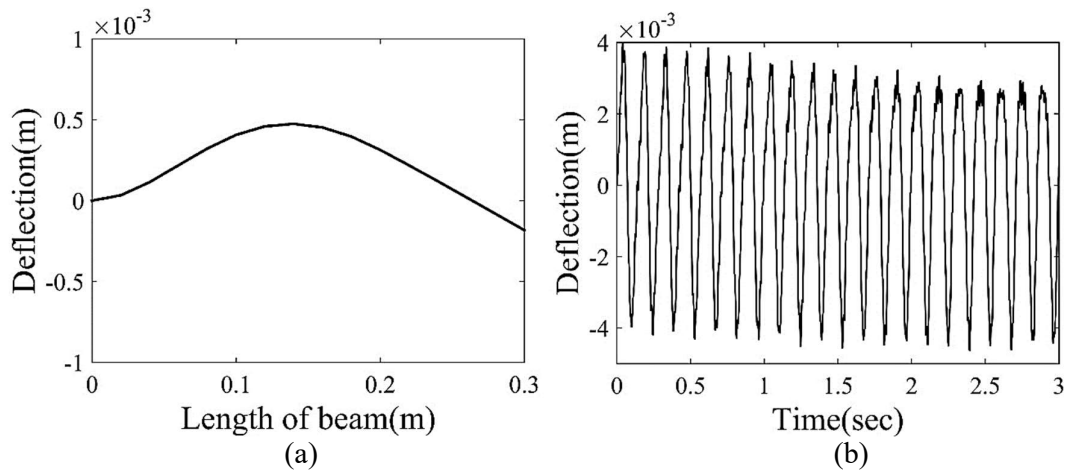
**Figure 4.10 (a) Mode of vibration (b) Time response graph (c) frequency spectrum**

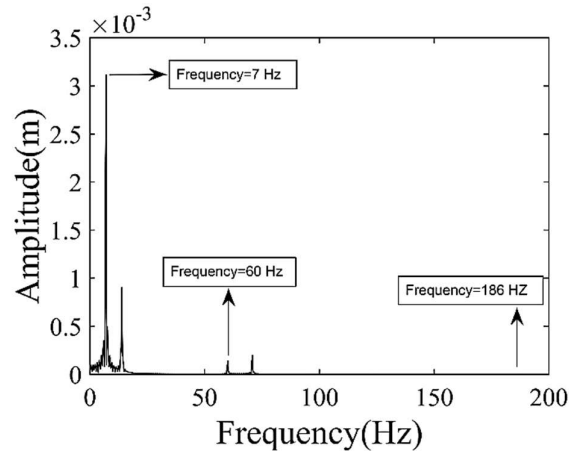
The dynamic response of cantilevered beam is calculated by giving the mixed excitation frequency of 60Hz and 186 Hz nearly the second and third natural frequency of the beam calculated above as shown in Table 4.2. The cantilevered beam is entirely excited in mixed mode of vibration. In Figure 4.10(a) the mode shape of the beam is shown. The time response at the tip of the cantilevered beam is investigated shown in Figure 4.10(b). Frequency spectrum of the time response signal at the tip of the beam is also obtained shown in Figure 4.10(c). from the above figures it is seen that the cantilevered beam is entirely vibrates in the mixed mode of vibration by giving the frequency of 60 Hz and 186 Hz.



**Figure 4.11 Actual dynamic response of beam with two mixed frequencies**

Where Figure 4.11 depicts the actual dynamic response of beam with two mixed frequencies. In the same manner, to simulate the exact effect of flow induced vibration the three modal frequencies are given as mixed excitation frequencies which is nearly first, second and third natural frequencies as shown in Table 4.2. Figure 4.11(a)-(c) shows the mode shape, time history and frequency spectrum of the beam vibration for an excitation of  $F = A \sin(2\pi \cdot 7t) + A \sin(2\pi \cdot 60t) + A \sin(2\pi \cdot 186t)$ , where  $A$  is the excitation amplitude and the beam is excited at three modal natural frequencies i.e. 7 Hz, 60 Hz and 186 Hz frequency. The figure indicates that the deflection shape of the beam is close to the mix bending mode of the beam. The frequency spectrum indicates three peaks corresponding to 7 Hz, 60 Hz and 186 Hz which are corresponding to excitation, first, second and third modal frequency.





(c)

**Figure 4.12 (a) Mode of vibration (b) Time response graph (c) frequency spectrum**

The dynamic response of cantilevered beam is calculated by giving the mixed excitation frequency of 7 Hz, 60Hz and 186 Hz nearly the first, second and third natural frequency of the beam calculated above as shown in Table 4.2. The cantilevered beam is entirely excited in mixed mode of vibration. In Figure 4.12(a) the mode shape of the beam is shown. The time response at the tip of the cantilevered beam is investigated shown in Figure 4.12(b). Frequency spectrum of the time response signal at the tip of the beam is also obtained shown in Figure 4.12(c). From the above figures it is seen that the cantilevered beam is entirely vibrates in the mixed mode of vibration by giving the frequency of 7 Hz 60 Hz and 186 Hz.

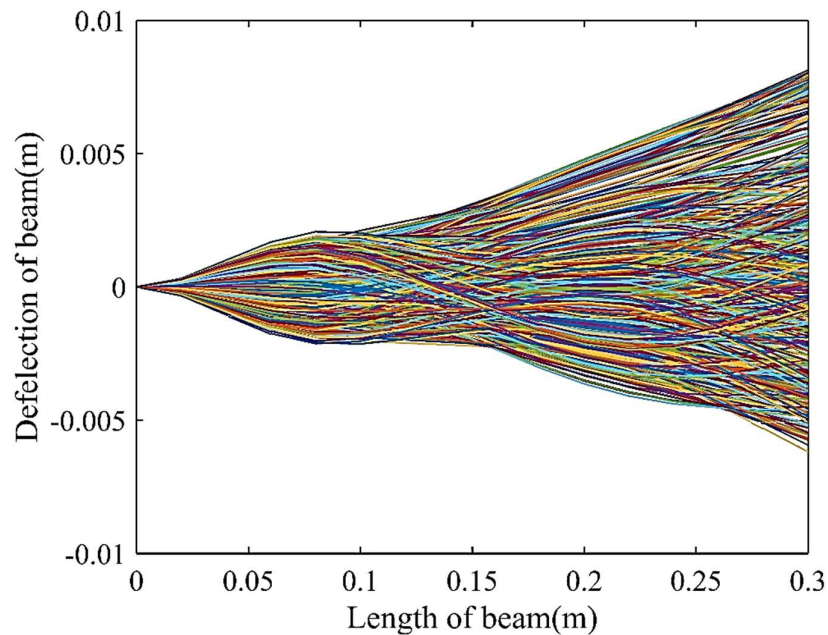


**Figure 4.13 Actual dynamic response of the beam with 3 mixed frequencies excitation**

Where Figure 4.13 depicts the actual dynamic response of beam with three mixed frequencies.

## 4.1 Estimation of Charge Generation

The mathematical modelling is purposed and the developed solution methodology is implemented in this section to estimate the charge generation from the deflection of cantilevered beam with piezoelectric material patch. In this section, estimation of charge generation from the dynamic response of beam is obtained by placing the piezoelectric material patch on the tip of the cantilever beam as shown in Figure 4.12.

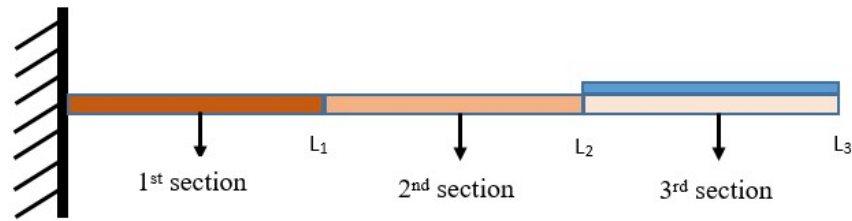


**Figure 4.12 Cantilevered stepped beam**

The piezoelectric material patch is placed on the tip of the cantilevered beam and the amount of charge generation is investigated shown in Figure 4.12. Firstly, the strain is calculated along the length ( $L_2$  to  $L_3$ ) of the third section of the beam where piezoelectric material patch is bonded.

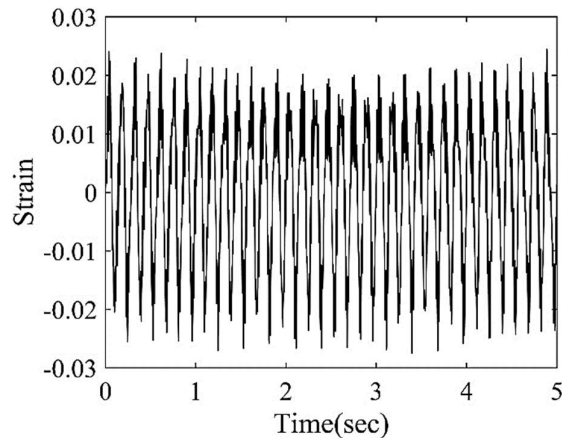


**Figure 4.13 Strain produced along the beam during deflection**

The strain along the length of the third section of the equivalent beam is studied as shown in Figure 4.13. Then, the linear piezoelectric theory is employed and integrated over the entire length of the 3<sup>rd</sup> section ( $L_2$  to  $L_3$ ). Therefore, the root mean square value of the corresponding charge generated is calculated i.e.  $2.21\text{E-}04$ .

## 4.2 Optimal Position of the Piezoelectric Patch Material Where Maximum Charge Generation Obtained

In this section, the same methodology is adopted as discussed in previous sections to investigate the optimal position of the piezoelectric patch material where maximum charge generation is obtained

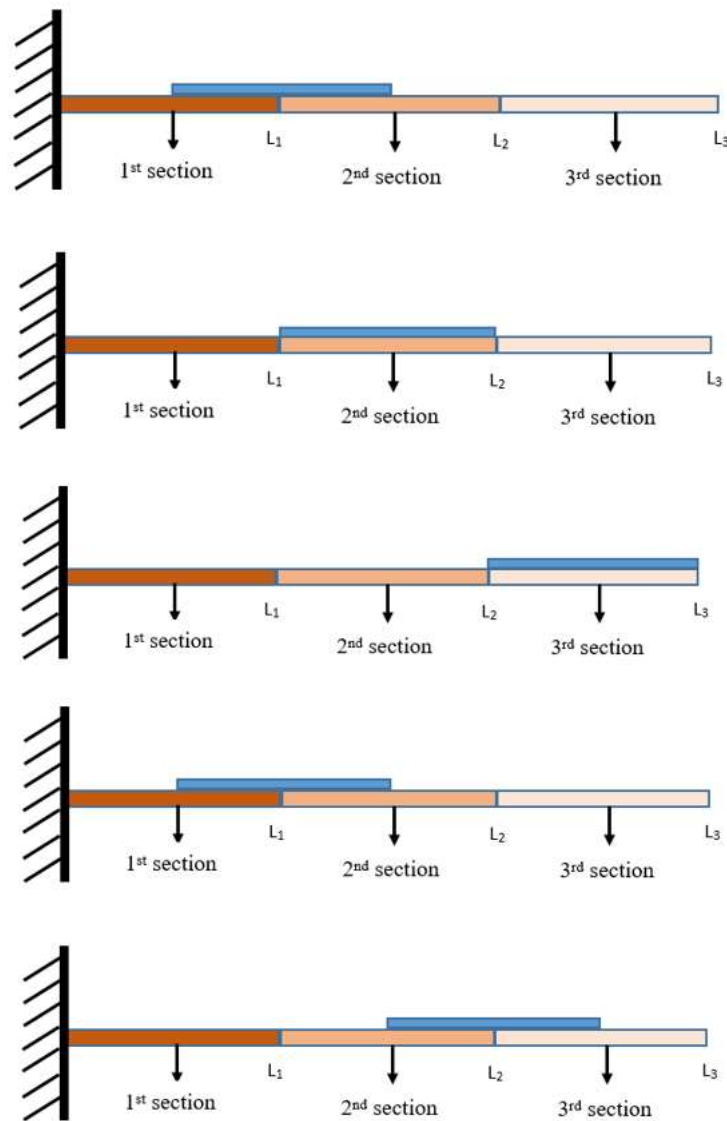
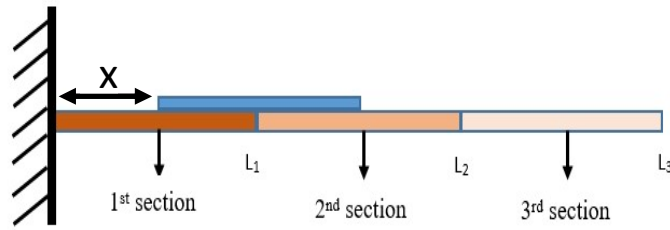


**Figure 4.14 Various location of PZT-patch**

Therefore, the developed methodology is applied on various locations of the piezoelectric patch as shown in Figure 4.14. to investigate the optimal position for maximum charge generation.



For estimating the charge at various locations of piezo-patch on the cantilvered beam, a distance  $x$  is varied where distance  $x$  is the distance of the piezoelectric patch from the fixed end of the cantilvered beam. Where Table 4.4 describes the amount of the charge generation at various location of piezo-patch by varying the distance of piezo-patch from fixed end of cantilvered beam.

**Table 4.4 shows the amount of Charge generation**

Sr No.	Position of piezo-patch When $x=$	Charge in microcoulombs ( $\mu\text{C}$ )
1.	0.04	2.42e-04
2.	0.08	2.35e-04
3.	0.10	0.0052
4.	0.14	3.25e-04
5.	0.18	1.92e-04
6.	0.20	2.21e-04

Table 4.4 depicts the amount of charge generated with piezoelectric patch placed at various location of the patch on the cantilvered beam. Figure 4.16 shows the variation of chagergeneration with respect to the position of the patch. From the results it has been concluded that when the piezoelectric patch material is bonded in the middle (0.1m from the fixed end) of the cantilvered beam. It may be noted that these results are generated for an excitationapplied at 0.06m from the free end. It is observed that if the position of the excitation pointchanges, quantity of charge generation changes. However, it is observed that for different

excitation position, maximum charge generated corresponding to same position (0.1m).

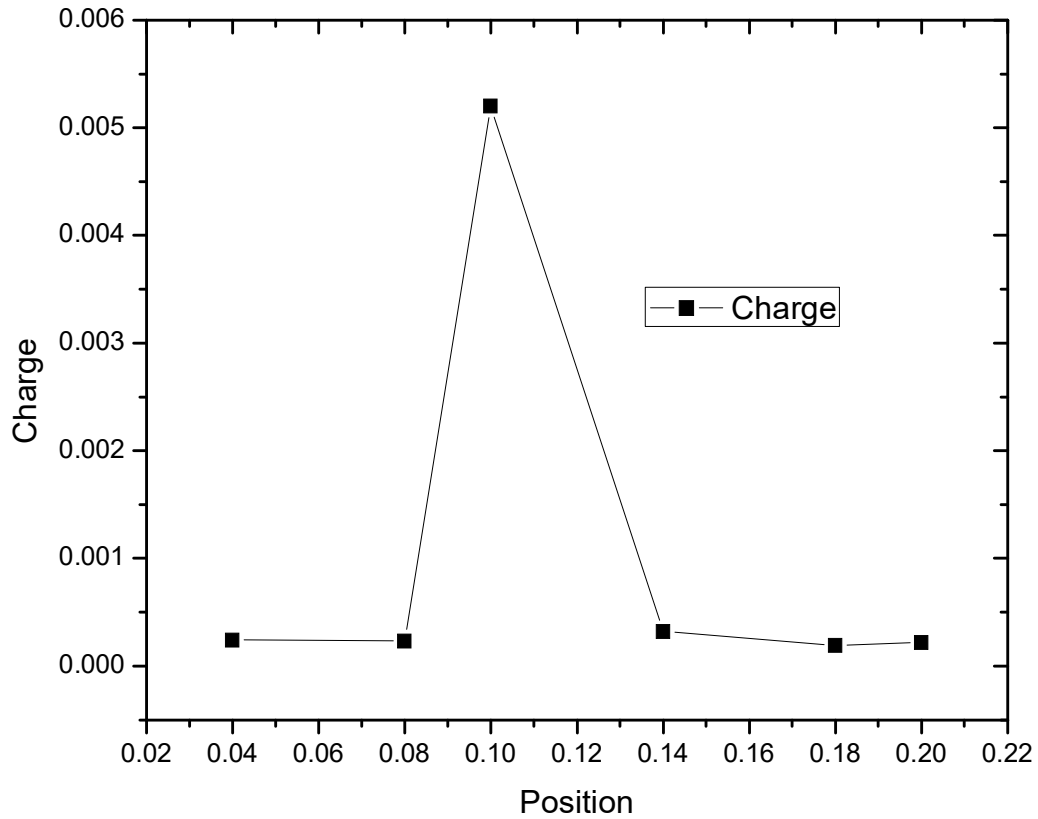


**Figure 4.16 Graph of charge against position of PZT-patch**

### Summary

The dynamic response of the cantilevered beam along with piezoelectric patch is obtained by using modal superposition method with Euler Bernoulli beam theory model. The strain and charge generated in piezo-patch by the dynamic response of cantilevered beam is calculated by using linear piezoelectric theory. In the same manner the charge generation is obtained by changing the position piezoelectric patch on the regular cantilevered beam. From the result discussed above, it has been concluded that the optimal placement of the piezo-patch is middle on the regular cantilevered beam where the maximum charge generation takes place.

## CHAPTER 5

### **CONCLUSIONS AND SCOPE FOR FUTURE WORK**

---

#### 5.1 Conclusions

The dynamics of piezoelectric cantilevered beam at higher bending modes of vibration for wind energy harvesting is investigated. A general MATLAB code was formulated on the basis of mathematical modelling developed. With the purposed MATLAB code in house the dynamic response of cantilevered beam along with piezoelectric patch was obtained. Further, the charge was obtained from the piezoelectric material patch. The parametric study is done for the various position of the piezoelectric material patch on the cantilever beam and optimal position of piezo-patch for maximum charge generation is also investigated. On the basis of the present work, the following conclusion can be done:

1. The dynamic response of cantilevered beam along with piezoelectric material patch is obtained at higher bending modes of vibration by using modal super-position method.
2. The strain developed in the cantilevered beam during the higher bending modes of vibration is calculated.
3. Further, the developed strain is used to calculate the charge generation with piezoelectric material patch is also calculated.
4. Optimal placement of the PZT-patch is also investigated where the maximum charge generation takes place.
5. It has been concluded that the middle position is the optimal placement of piezoelectric material layer.

Following publication are communicated on the basis of present thesis:

1. Singh R, Purohit A and Kumar R. Dynamics of Piezoelectric Cantilevered Beam at higher bending mode for wind Energy Harvesting Symposium and Workshop for Analytical Youth on Applied Mechanics 2018 (SWAYAM) BITS Pilani, K. K. Birla Goa Campus. (Accepted)

## 5.2 Scope for The Future Work

1. The present methodology can be applied for uneven structures or shapes such as aerofoil geometry and plates.
2. Different materials of structure and PZT-patch can also be considered for energy harvesting or MEMS technology.
3. The flow term in the form of pressure and velocity can also be applied for exciting the structure to investigate the dynamic response.

## References

- Akaydin, H. D., Elvin, N., and Andreopoulos, Y. (2010). Energy harvesting from highly unsteady fluid flows using piezoelectric materials. *Journal of Intelligent Material Systems and Structures*, 21(13), 1263-1278.
- Akaydin, H. D., Elvin, N., and Andreopoulos, Y. (2010). Power extraction from highly unsteady fluid flows using piezoelectric generators. *Journal of Intelligent Material Systems and Structures*, 21(13), 1263-1278.
- Allen, J. J., and Smits, A. J. (2001). Energy harvesting eel. *Journal of fluids and structures*, 15(3-4), 629-640.
- Bailey, T., and Hubbard, J. E. (1985). Distributed piezoelectric-polymer active vibration control of a cantilever beam. *Journal of Guidance, Control, and Dynamics*, 8(5), 605-611.
- Balint, T. S., and Lucey, A. D. (2005). Instability of a cantilevered flexible plate in viscous channel flow. *Journal of Fluids and Structures*, 20(7), 893-912.
- Bilgen, O., Ali, S. F., Friswell, M. I., Litak, G., and de Angelis, M. (2013). Non-linear piezoelectric vibration energy harvesting from a vertical cantilever beam with tip mass. In *ASME 2013 Conference on Smart Materials, Adaptive Structures and Intelligent Systems* (pp. V001T04A008-V001T04A008). American Society of Mechanical Engineers.
- Eloy, C., Lagrange, R., Souilliez, C., and Schouveiler, L. (2008). Aeroelastic instability of cantilevered flexible plates in uniform flow. *Journal of Fluid Mechanics*, 611, 97-106.
- Erturk, A., and Inman, D. J. (2009). An experimentally validated bimorph cantilever model for piezoelectric energy harvesting from base excitations. *Smart materials and structures*, 18(2), 025009.
- Friswell, M. I., Ali, S. F., Bilgen, O., Adhikari, S., Lees, A. W., and Litak, G. (2012). Non-linear piezoelectric vibration energy harvesting from a vertical cantilever beam with tip mass. *Journal of Intelligent Material Systems and Structures*, 23(13), 1505-1521.
- Godara, R. K., and Joglekar, M. M. (2015). Mitigation of residual oscillations in electrostatically actuated microbeams using a command-shaping approach. *Journal of Micromechanics and Microengineering*, 25(11), 115028.

Godara, R. K., and Joglekar, M. M. (2017). Alleviation of residual oscillations in electrostatically actuated variable-width microbeams using a feedforward control strategy. *Microsystem Technologies*, 23(10), 4441-4457.

Godara, R. K., and Joglekar, M. M. (2018). Suppression of contact bounce in beam-type microelectromechanical switches using a feedforward control scheme. *Journal of Vibration and Control*, 1077546318755978.

Huang, L. (1995). Flutter of cantilevered plates in axial flow. *Journal of Fluids and Structures*, 9(2), 127-147.

Izadgoshasb, I., Lim, Y. Y., Lake, N., Tang, L., Padilla, R. V., and Kashiwao, T. (2018). Optimizing orientation of piezoelectric cantilever beam for harvesting energy from human walking. *Energy Conversion and Management*, 161, 66-73.

Jang, S. K., and Bert, C. W. (1989). Free vibration of stepped beams: exact and numerical solutions. *Journal of Sound Vibration*, 130, 342-346.

Kisa, M., and Gurel, M. A. (2007). Free vibration analysis of uniform and stepped cracked beams with circular cross sections. *International Journal of Engineering Science*, 45(2-8), 364-380.

Kumar, S., Srivastava, R., and Srivastava, R. K. (2016). Design and analysis of smart piezo cantilever beam for energy harvesting. *Ferroelectrics*, 505(1), 159-183.

Leung, R. C. K., and So, R. M. C. (2001). Noise generation of blade–vortex resonance. *Journal of sound and vibration*, 245(2), 217-237.

Lu, F., Lee, H. P., and Lim, S. P. (2003). Modelling and analysis of micro piezoelectric power generators for micro-electromechanical-systems applications. *Smart Materials and Structures*, 13(1), 57.

Paidoussis, M. P. (1998). *Fluid-structure interactions: slender structures and axial flow* (Vol. 1). Academic press.

Rao, S. S., and Fook Fah. Yap. *Mechanical Vibrations*. Prentice Hall, 2011

Tang, L., Païdoussis, M. P., and Jiang, J. (2009). Cantilevered flexible plates in axial flow: energy transfer and the concept of flutter-mill. *Journal of Sound and Vibration*, 326(1-2), 263-276.

Vaz, J. D. C., and De Lima Junior, J. J. (2016). Vibration analysis of Euler-Bernoulli beams in multiple steps and different shapes of cross section. *Journal of Vibration and Control*, 22(1), 193-204.

Wang, Q., and Wang, C. M. (2000). Optimal placement and size of piezoelectric patches on beams from the controllability perspective. *Smart Materials and Structures*, 9(4), 558.

Wu, H., Tang, L., Yang, Y., and Soh, C. K. (2014). Development of a broadband nonlinear two-degree-of-freedom piezoelectric energy harvester. *Journal of Intelligent Material Systems and Structures*, 25(14), 1875-1889.

ORIGINALITY REPORT

---

15%

SIMILARITY INDEX

5%

INTERNET SOURCES

15%

PUBLICATIONS

2%

STUDENT PAPERS

---

PRIMARY SOURCES

---

1

ijret.org

Internet Source

2%

2

S.K. Jang, C.W. Bert. "Free vibration of stepped beams: Exact and numerical solutions", Journal of Sound and Vibration, 1989

Publication

2%

3

Vinod R Challa. "A vibration energy harvesting device with bidirectional resonance frequency tunability", Smart Materials and Structures, 02/01/2008

Publication

2%

4

Huseyin Dogus Akaydin, Niell Elvin, Yiannis Andreopoulos. "Energy Harvesting from Highly Unsteady Fluid Flows using Piezoelectric Materials", Journal of Intelligent Material Systems and Structures, 2010

Publication

1%

5

Foda, M.A.. "Vibration confinement in a general beam structure during harmonic excitations", Journal of Sound and Vibration, 20060822

Publication

1%

6	Q Wang. Smart Materials and Structures, 08/2000 Publication	1%
7	R. K. Godara, M. M. Joglekar. "Alleviation of residual oscillations in electrostatically actuated variable-width microbeams using a feedforward control strategy", Microsystem Technologies, 2016 Publication	1%
8	<a href="http://www.me.berkeley.edu">www.me.berkeley.edu</a> Internet Source	1%
9	F Lu. "Modeling and analysis of micro piezoelectric power generators for micro-electromechanical-systems applications", Smart Materials and Structures, 02/01/2004 Publication	1%
10	Balint, T.S.. "Instability of a cantilevered flexible plate in viscous channel flow", Journal of Fluids and Structures, 200510 Publication	<1%
11	A Erturk. "An experimentally validated bimorph cantilever model for piezoelectric energy harvesting from base excitations", Smart Materials and Structures, 02/01/2009 Publication	<1%
12	Tang, L.. "The influence of the wake on the	

---

stability of cantilevered flexible plates in axial flow", Journal of Sound and Vibration, 20080219

Publication

<1%

---

13

T.X. Yu, XinMing Qiu. "Mode Technique, Bound Theorems, and Applicability of the Rigid-Perfectly Plastic Model", Wiley-Blackwell, 2017

Publication

<1%

---

14

Tang, Lihua, and Yaowen Yang. "A nonlinear piezoelectric energy harvester with magnetic oscillator", Applied Physics Letters, 2012.

Publication

<1%

---

15

TAKIGAMI, Tadao, Takahiro TOMIOKA, and Joel HANSSON. "Vibration Suppression of Railway Vehicle Carbody with Piezoelectric Elements", Journal of Advanced Mechanical Design Systems and Manufacturing, 2007.

Publication

<1%

---

16

[www.citeulike.org](http://www.citeulike.org)

Internet Source

<1%

---

17

Submitted to Loughborough College

Student Paper

<1%

---

18

Khalid, Anam, Amit Kumar Redhewal, Manoj Kumar, and Anupam Srivastav. "Piezoelectric Vibration Harvesters Based on Vibrations of Cantilevered Bimorphs: A Review", Materials Sciences and Applications, 2015.

<1%

19 Icardi, Ugo, Marco Di Sciuva, and Liviu I. Librescu. "", Smart Structures and Materials 1998 Mathematics and Control in Smart Structures, 1998.

Publication

---

20 eprints.utm.my <1 %

Internet Source

---

21 Gorman, D.J.. "Free vibration analysis of the completely free rectangular plate by the method of superposition", Journal of Sound and Vibration, 19780408

Publication

---

22 CHRISTOPHE ELOY. "Aeroelastic instability of cantilevered flexible plates in uniform flow", Journal of Fluid Mechanics, 09/2008

Publication

---

23 Submitted to University of Nottingham <1 %

Student Paper

---

24 Submitted to iGroup <1 %

Student Paper

---

25 Submitted to Sahyadri College of Engineering and Management <1 %

Student Paper

---

26 Pilkey, D.F.. "High performance computing issues for model reduction/expansion", <1 %

27

[ethesis.nitrkl.ac.in](http://ethesis.nitrkl.ac.in)

Internet Source

<1%

---

28

Lihua Tang, Yaowen Yang. "A nonlinear piezoelectric energy harvester with magnetic oscillator", Applied Physics Letters, 2012

Publication

<1%

---

Exclude quotes      On

Exclude matches      < 10 words

Exclude bibliography      On